NAVAL POSTGRADUATE SCHOOL
Monterey, California

THESIS

DYNAMICS OF AN ERICA CYCLONE

by

Amy E. Chalfant

June 1989

Thesis Advisor Carlyle H. Wash

REPORT DOCUMENTATION PAGE

1a Report Security Classification: Unclassified		1b Restrictive Markings	
2a Security Classification Authority		3 Distribution Availability of Report: Approved for public release; distribution is unlimited.	
2b Declassification Downgrading Schedule			
4 Performing Organization Report Number(s)		5 Monitoring Organization Report Number(s)	
6a Name of Performing Organization: Naval Postgraduate School	6b Office Symbol (*if applicable*): 35	7a Name of Monitoring Organization: Naval Postgraduate School	
6c Address (*city, state, and ZIP code*): Monterey, CA 93943-5000		7b Address (*city, state, and ZIP code*): Monterey, CA 93943-5000	
8a Name of Funding Sponsoring Organization	8b Office Symbol (*if applicable*)	9 Procurement Instrument Identification Number	
8c Address (*city, state, and ZIP code*)		10 Source of Funding Numbers	
		Program Element No	Project No / Task No / Work Unit Accession No

11 Title (*Include security classification*): DYNAMICS OF AN ERICA CYCLONE

12 Personal Author(s): Amy E. Chalfant

13a Type of Report	13b Time Covered	14 Date of Report (*year, month, day*)	15 Page Count
Master's Thesis	From To	June 1989	65

16 Supplementary Notation: The views expressed in this thesis are those of the author and do not reflect the official policy or position of the Department of Defense or the U.S. Government.

17 Cosati Codes			18 Subject Terms (*continue on reverse if necessary and identify by block number*)
Field	Group	Subgroup	Rapid cyclogenesis, ERICA

19 Abstract (*continue on reverse if necessary and identify by block number*)

Cyclogenesis is studied during Intensive Observation Period (IOP) 2 from the Experiment on Rapidly Intensifying Cyclones over the Atlantic (ERICA) conducted in Winter 1988-89. The detailed synoptic discussion outlines the development of multiple cyclones in the western North Atlantic Ocean. The surface analyses with data included from ships, buoys, and east coast U.S. land stations resolve a dramatic rapid development case with a deepening rate of 30 mb/12 h. A comparison of observed events with operational NMC Nested Grid Model and Global Spectral Model forecasts revealed skillful overall performance, however there were some deficiencies in handling details of the cyclogenesis event. Diagnostics of the case show destabilization occurring during the pre-cyclogenesis period and strong upper-level forcing for the rapidly developing center.

20 Distribution Availability of Abstract	21 Abstract Security Classification	
☒ unclassified unlimited ☐ same as report ☐ DTIC users	Unclassified	
22a Name of Responsible Individual: Carlyle H. Wash	22b Telephone (*include Area code*): (408) 646-2044	22c Office Symbol: 63Wx

DD FORM 1473,84 MAR — 83 APR edition may be used until exhausted; All other editions are obsolete

Approved for public release; distribution is unlimited.

Dynamics of an ERICA cyclone

by

Amy E. Chalfant
Captain, United States Air Force
B.S., Old Dominion University, 1983

Submitted in partial fulfillment of the
requirements for the degree of

MASTER OF SCIENCE IN METEOROLOGY

from the

NAVAL POSTGRADUATE SCHOOL
June 1989

Author: Amy E. Chalfant

Amy E. Chalfant

Approved by: Carlyle H. Wash

Carlyle H. Wash, Thesis Advisor

Wendell Nuss, Second Reader

Robert J. Renard, Chairman,
Department of Meteorology

Gordon E. Schacher,
Dean of Science and Engineering

TABLE OF CONTENTS

LIST OF TABLES

LIST OF FIGURES

ACKNOWLEDGEMENTS

I would like to thank Professor Carlyle Wash for his assistance and support he readily gave me for completing this thesis. I would also like to express appreciation to Prof. W. Nuss for imparting his first-hand knowledge of IOP-2 which aided immeasurabely in the analysis of the storms and for his comments as second reader on this thesis. Finally, I thank my husband, Bob, for his love and support during my tour at the Naval Postgraduate School.

I. INTRODUCTION

Coastal and maritime rapid cyclogenesis is a serious problem for commerce and safety due to the destructive nature of these storms. Recently, considerable research has been undertaken to understand the intensification processes including studies to improve forecasting of these events. The definition of rapid cyclogenesis is that the central pressure falls 24 mb in 24 hours (Sanders and Gyakum, 1980) at 60°N. It is geostrophically corrected for other latitudes (ϕ) by multiplying the deepening rate by $(\frac{\sin \phi}{\sin 60°})$. Sanders and Gyakum indicate these cyclones are cold season, maritime events with maximum frequency in January and February. These rapidly deepening storms often are found to be coincident with the strong temperature gradients of the Kurishio current east of Japan and the Gulf Stream current east of the United States.

Numerical models consistantly underforecast rapid cyclogenesis. Even the new Nested Grid Model (NGM) forecasts explosive cyclogenesis less frequently than observed, particularly at longer time ranges and the model generally underdeepens these cyclones (Sanders, 1987). The lack of understanding of the mechanisms for rapid cyclogenesis contributes to our inability to correct these numerical model weaknesses. This has led to studies of rapid cyclogenesis in which the primary objective is to improve the model forecasting ability.

In 1986, the Genesis of Atlantic Lows Experiment (GALE) was conducted to study rapid cyclogenesis on the east coast of the United States. The synoptic scale objectives of the experiment were to study the physical processes of developing cyclones, describe the airflow and moisture patterns, and develop and test numerical prediction models to model east coast rapidly intensifying cyclones (Dirks, 1988). Important preliminary findings from numerous studies are that rapid cyclogenesis is a scale interaction problem in which mesoscale and synoptic scale events are important to the development. For the rapid cyclogenesis that occurred during GALE, certain mesoscale events occurred in concert, including offshore latent heat release, cold air damming, and coastal frontogenesis. Modified regional forecast models that were tested against GALE Intensive Observation Periods (IOPs) showed improvements in forecasting east coast rapid cyclogenesis (Dirks, 1988).

The Experiment on Rapidly Intensifying Cyclones over the Atlantic (ERICA) was conducted from 1 December 1988 to 1 March 1989 with the objectives of understanding

the physical processes leading to rapid cyclogenesis and improving numerical model forecasts of rapid cyclogenesis. Understanding the events leading up to a rapidly deepening storm and improving the initilization of models should increase the forecast accuracy of these events. Because the rapid cyclogenesis is mainly a maritime event, observations of explosive cyclones have been very limited. ERICA was designed to increase observations of rapid cyclogenesis through the use of aircraft, increased rawinsonde soundings, buoys, ships, satellite imagery, and radars with joint participation from NOAA, DoD, and various universities.

The area of interest extends from approximately 40°N to 47°N between 59°W to 69°W and is centered on the climatologically favored area for rapid cyclogenesis. During a cyclogenesis event data from all sources was gathered for real-time forecasting and post-storm analysis. Air Force aircraft provided cyclone-scale data around the outer radii of the storm including dropsondes, while the NCAR Sabreliner provided data of the structure of the disturbance in the upper troposphere and lower stratosphere up to 13 km as well as verifying remote sensing techniques. The satellite imagery from the geostationary satellite provided observations over water every 30 minutes showing the large scale cloud patterns evolving with the deepening storm. A Navy P-3 deployed the original fifty drifting buoys at 200 km spacing and reseeded the buoy field as required during the ERICA project. NOAA aircraft were deployed 6 to 12 hours before the storm was predicted to rapidly deepen and focused on the meso-alpha and meso-beta scale storm structures.

Along with moored buoys and the Coastal-Marine Automated Network Stations, 50 drifting buoys were dropped into a network spaced approximately every 200 km through the ERICA region. The buoys, communicating by satellite, drift with the ocean current reporting mean sea level pressure, air temperature, and sea temperature hourly to provide increased surface data coverage of the ERICA region. Additional buoys were used to reseed the storm region as the original buoys periodically failed.

This thesis will use all available operational data to investigate and explain the behavior of a rapidly developing cyclone that occurred during 13-14 December 1988, which is the second intensive observation period (IOP-2). The thesis focuses on IOP-2 and is intended as a first look at storm development and intensification. The IOP-2 numerical model predictions are compared to observations to determine the events that each model failed to forecast. Grid point data from the NMC Spectral Model are analyzed to dynamically explain cyclone development following quasi-gestrophic theory. The hypothesis in previous studies has been that rapid cyclogenesis occurs when upper-level and

lower-level forcing, low static stability, and a pre-existing surface disturbance occur simultaneously. Relating this theory to IOP-2, Spectral Model gridded analyses are used to estimate the various forcing mechanisms and the static stability in an effort to study this hypothesis. Since this is a preliminary study, events which are not explained from the data will be documented for further research.

The research into IOP-2 is divided into sections describing the synoptic development of IOP-2, the model performance, the dynamics of the cyclone, and the conclusions and recommendations. The thesis begins with a brief literature review of rapid cyclogenesis, where only several key recent articles on aspects of rapid cyclogenesis are summarized. An overview of the synoptic events are in Chapter 3. Chapter 4 is a model summary of the Nested Grid Model and the Spectral Model's performance during IOP-2. The dynamic aspects of IOP-2 are explained in Chapter 5. The conclusions and recommendations are in Chapter 6.

II. BACKGROUND

Numerous recent studies have investigated various aspects of rapid cyclogenesis. Three relevant papers are reviewed, in which past and current numerical model performance and the important processes in rapid cyclogenesis are studied. Sanders and Gyakum (1980) describe the climatological regions and the synoptic pattern associated with a high incidence of rapid cyclogenesis. Sanders and Gyakum studied a three-year sample of storms in both the North Atlantic and Eastern Pacific Oceans where the deepening rate is greater than or equal to 1 mb/hr for 24 h, which is also referred to as a deepening rate of one bergeron. The study excluded May-August, when the frequency of rapid cyclogenesis is very small. The maximum occurrence was found in the winter season with the greatest frequency in January. The number of explosive cyclones is greater in the North Pacific Ocean, although the number of intense cyclones with deepening rates greater than 2.0 bergerons is greater in the North Atlantic Ocean.

The relationship between the 500 mb shortwave trough and the rapidly deepening cyclones was explored by Sanders and Gyakum (1980). During a period of seven days, the shortwave trough was found south and west of the explosively deepening cyclone surface low pressure centers. In a sample of 252 cases, the average distance from the surface cyclone center to the trough at 500 mb was approximately 400 n mi to the west-southwest. This relationship between 500 mb and the surface suggests that rapidly deepening cyclones have strong baroclinicity associated with them. The strong sea surface temperature (SST) gradient also may play a role in the development of the storm due to strong sensible and latent heat fluxes as cold continental air moves over the warmer SST. This suggests that explosive cyclones have significant diabatic heating associated with them as well. Explosive cyclogenesis is found over a large range of SSTs and the authors concluded they are not sensitive to the magnitude of SST as found for tropical cyclones.

Also discussed are the past numerical models' skill in forecasting rapid cyclogenesis. NMC numerical model prediction of rapid cyclogenesis was found to drastically underforecast the intensity of the cyclones. Decreasing the horizontal grid length by 1/2 resulted in only a 10% decrease in model error. The model forecast position of the storms are generally south and west of the observed cyclone position. A possible source for error in the model, suggested by Sanders and Gyakum, is an inadequate represen-

tation of the bulk effects of cumulus convection. Since the SST gradient is also an important factor in rapid cyclogenesis, the planetary boundary layer and vertical resolution in the model are also sources of error.

In a more recent article, Sanders (1987) explored the Nested Grid Model (NGM) and Spectral Model explosive cyclogenesis forecasting capability for the period 1 September 1986 to 31 April 1987. Cyclogenesis in the model was found in regions where climatology indicates rapid deepening predominantly occurs. The rapidly deepening cyclones were found more frequently in the analysis than in the forecasts for both models. For example, 22 cyclones with deepening rates greater than 20 mb in 12 h were observed in the NGM analysis. Of the 22, five instances of explosive deepening were predicted in the 12-h forecasts, six in the 24-h forecasts, four in the 36-h forecasts, and only two in the 48-h forecasts. Sanders indicated that more study is required to determine the nature of the decreased prediction rate at the longer forecast periods. Many storms were not forecast by the model, along with occasional false alarms. Both models were less effective in forecasting rapid cyclogenesis in the eastern North Pacific Ocean than in the North Atlantic Ocean. The problem with prediction of rapidly deepening cyclones in the North Pacific Ocean may be due to fewer observations by ships, aircraft, and poorer satellite coverage. Therefore, the initial conditions are not as well known and accurate upwind conditions are unavailable, unlike in the North Atlantic Ocean region.

In 1986, during the early period of NGM use, its performance was found by Sanders (1987) to be no better than the earlier Limited Fine Mesh Model (LFM), although the sample size for part of this study was small. Changes in 1987 to the NGM produced an improved first guess and used satellite soundings more effectively. Subsequent changes in the model, producing better precipitation prediction and boundary layer diurnal variation over land, improved forecasts over the ocean as well. Problems still exist in forecasting rapid cyclogenesis where the grids overlap. The highest resolution grid within the NGM is the C-grid with a grid spacing of 90 km. This grid is centered on North America and ends just off the east coast. A coarser B-grid of 180 km spacing is used for the western North Atlantic and eastern North Pacific Ocean. The area where these grids merge is where additional problems forecasting rapid cyclogenesis occur. To correct this problem, Sanders suggests increasing the area covered by the fine mesh, although the computation increase would be considerable. The forecast of rapid cyclogenesis was found to be greater when the storm was in the fine C-grid mesh, but it also produces a larger false alarm rate. The false alarm rate is greater in the North Pacific Ocean. The

model overpredicted explosive cyclogenesis occurring over North America, which Sanders indicated was probably a systematic error in the model.

The Spectral Model was found to perform less well in the North Pacific Ocean than in the North Atlantic region. A number of successes were found in the Pacific region when the storms were close to the west coast of the U.S. and in the Gulf of Alaska. The success in this region may be due to an improved initial analysis provided by the increased data available due to the rawinsonde network. The results from the Spectral Model indicates an improvement over the LFM performance. Evaluating the Spectral Model only over regions of previous LFM study, the improvement in the Spectral Model is even more pronounced.

Sanders concluded that although these models have limitations, the skill in predicting rapid cyclogenesis has improved. Results from the study indicate that no one physical process is missing for today's oceanic cyclogenesis forecast model. The key research problem is still to improve the skill of forecasting rapid cyclogenesis and to extend the range of predictability of these events.

In the third paper Uccellini (1989) reviews results from a number of studies on the rapid cyclogenesis problem. The rapid deepening phase of the storm occurs over only a short period of time of the entire development cycle of the storm. The physical and dynamical processes leading to rapid cyclogenesis are a combination of many events which may be present in the development of all cyclones, but are especially efficient in development for an explosive cyclogenesis event.

Upper level conditions that are important in rapid cyclogenesis are divergence, vorticity advection, and jet streaks. Surface cyclones develop in response to divergence aloft and convergence at the surface. Divergence aloft can be inferred from the vorticity and thermodynamic equations. Positive vorticity advection is often used to approximate the divergence and serves as a signature of divergence required for surface cyclone development. In previous studies (Sanders and Gyakum, 1980), the 500 mb shortwave trough is found approximately 500 km upstream from the surface cyclogenesis region. Another source for divergence aloft is the entrance and exit regions of the jet streak.

Tropopause folds and potential vorticity also can contribute to rapid cyclogenesis. A tropopause fold occurs as stratosphere air extends into the upper tropospheric baroclinic zones below the normal tropopause height. Uccellini states that in many cases a tropopause fold and surface cyclogenesis occur simultaneously. During a tropopause fold, high static stability stratospheric air is forced into the upper

troposphere. If potential vorticity, $PV = -(\xi + f)\frac{\partial \theta}{\partial p}$, is conserved, stretching and destabilization of the airmass will result in an increase in vorticity.

In the President's Day storm analysis, high potential vorticity air was also depicted by a model at low levels. Due to latent heat release in a low-level baroclinic zone, high potential vorticity can be created at low levels and induce cyclogenesis upward through the troposphere. The low- level potential vorticity center must occur downwind of the upper-level potential vorticity center to create a positive feedback between the two. The cyclonic vorticity through the atmosphere creates the pressure falls required for cyclonic development.

At low levels, the thermal advection pattern, sensible and latent heat fluxes and low static stability are important conditions which promote rapid cyclogenesis. The thermal pattern in explosive cyclogenesis usually has an 's' shape which is typical of many cyclones. The boundary layer latent and sensible heat fluxes due to cold air moving over the warmer ocean is also a mechanism leading to rapid cyclogenesis. The amount of influence by heat fluxes varies for each case. Various numerical models handle the boundary layer differently which affects their cyclone forecasts. The static stability also influences deepening rates and is dependent on boundary layer heating. Low static stability is an environment for more efficient forcing of upward vertical motion. This will enhance the low-level convergence and upper-level divergence during storm development (Wash et al., 1988).

Studies into rapid cyclogenesis have shown that many dynamic and thermodynamic processes are important to the cyclonic development. The processes are both upper and lower level and include positive vorticity advection, jet streaks, potential vorticity development at both the surface and in the area of the upper-level tropopause fold, thermal advection, and low static stability which enhances upward vertical motion and divergence aloft. The conditions producing rapid cyclogenesis are a mixture of these many physical processes which work together to create explosive deepening. Analysis of the physical processes which occurred in IOP-2 will help understand explosive cyclogenesis.

III. SYNOPTIC DISCUSSION

A. 0000 UTC 13 DECEMBER 1988

At the start of IOP-2, on 0000 UTC 13 December (hereafter, date and time will be denoted day/ time UTC, e.g., 13/0000), the National Meteorolgical Center (NMC) MSL pressure analysis of the surface pattern (Fig. 1) indicated multiple lows east of Florida centered approximately near 28°N, 77°W. These low pressure centers have a central pressure analyzed at 1010 mb. On the satellite image for the same time, the clouds are organized with a general cyclonic circulation centered on this low pressure region. To the north, a 1039 mb high pressure system is enlongated along the eastern seaboard from Maine to South Carolina. The 13/0000 UTC satellite image also shows low clouds prevalent off the coast in the high's anticyclonic circulation..

At 850 mb (not shown), a low is analyzed by the NMC Limited Fine Mesh (LFM) analysis just east of northern Florida. Associated with the low pressure pattern is a broad temperature gradient from 27° to 42°N over the western North Atlantic Ocean. This initial low east of Florida is centered on the southern portion of the broad baroclinic zone at 850 mb. To the west, a second sharp trough extends from Lake Superior to Missouri.

The 500 mb analysis for this time shows the trough associated with the surface low off of Florida lies from western North Carolina to the Gulf of Mexico. Height falls of 10 to 50 m are found over Florida, Georgia, and South Carolina. A second trough in the Midwest is significantly stronger with height falls over Michigan and Wisconsin of 110 m and shows a pronounced diffluent structure to its east.

At 300 mb, two strong jet streaks are analyzed, one off the east coast and the second over the Great Plains. The coastal surface low is located under the right rear entrance region of the eastern 300 mb jet, which is a divergence quadrant of the jet streak. The jet streak maximum winds are analysed to be 150 kt on the 300 mb chart, but no observations are available from the operational data to confirm this analysis. The left front exit region of Midwestern jet streak is favorably located over the midwestern 500 mb and surface troughs to support future development.

B. 1200 UTC 13 DECEMBER 1988

The surface analyses presented at 13/1200 UTC and subsequent times are subjective analyses utilizing operational and ERICA data that were not available in real-time.

Data sources include land stations, ship reports, and moored and drifting buoys. The surface analysis figures indicate only some of the data used in the analyses for clarity. By 13/1200 UTC the surface analysis (Fig. 2), including the ERICA drifting buoy data, shows the multiple center cyclone, analyzed twelve hours earlier, is resolved as one low located at 28°N, 72.5°W. This cyclone has a central pressure of 1004 mb, which is a conservative estimate considering the 20 kt wind east of the low center. A trough extends from the low northwestward toward eastern Massachusetts. The satellite image (Fig. 3) shows that the cyclone cloud area has grown and shows colder cloud tops than at 13/0000 UTC. A comma cloud appears on the satellite image near 34°N, 69°W. A comparison of the satellite data with the subjective MSL pressure analyses, complete with the drifting buoy and ship data, indicates no pressure minimum in this area and the comma cloud is associated with the upper-level forcing of the first shortwave trough. The coastal high has moved northeasterly to approximately 150 miles east of Nova Scotia and weakened to 1027 mb.

The NMC LFM 850 mb analysis (Fig. 4) shows the low pressure system is nearly closed off and a sharp trough, analyzed with observations from ERICA Air Weather Service (AWS) dropsondes, extends from the North Carolina coast to 25°N 70°W. As discussed earlier, a broad temperature gradient is analyzed between 25° to 45°N over the North Atlantic coast states eastward. The analysis shows that warm and cold temperature advection is very strong and the cyclone center is located on the warm side of the broad baroclinic zone.

At 500 mb (Fig. 5) the first shortwave is analyzed west of the surface cyclone off the southeast United States. The second shortwave moving eastward through the midwest is located on a line from Michigan to Georgia. Large height falls are still present in the upper midwest, with Dayton, Ohio reporting -140 m and Huntington, West Virginia dropping 160 m.

The NMC 300 mb analyses (Fig. 6) shows the eastern jet streak located from 35°N, 69°W northeastward off the chart. The divergence area in the right rear quadrant of the eastern jet streak is no longer near the surface low to support its development, although the divergent quadrant of the jet is over the comma cloud development at 69°W. The jet streak propogating through the central U.S. reaches Tennessee by this observation time with the analyzed maximum wind speed of 130 kt. Wind reports are missing in the jet core except for a 170 kt aircraft report which appears to have a 90° direction error relative to the surrounding reports and the 300 mb pattern.

Six hours later, 13/1800 UTC, the surface analysis (Fig. 7) shows the first low is now located at 30°N, 69°W. The central pressure is 1002 mb with a 6 h deepening rate of only 2 mb. By this time the surface analysis also shows a new center forming on the surface trough with a central pressure of 1005 mb in response to the upper-level forcing of the second shortwave trough as it approached the east coast. The satellite image (Fig. 8) shows cloud development east of Virginia over the past 6 h. Low clouds extend along the coast and are organized into cloud bands along the North and South Carolina coasts. The ERICA Field Summary (Hartnett et al., 1989) concludes the bands are due to sea-surface temperature gradients along the north wall of the Gulf Stream. The clouds associated with the first cyclone have warm tops and extend westward almost to the new coastal system.

C. 0000 UTC 14 DECEMBER 1988

The 14/0000 UTC subjective analysis (Fig. 9) shows the eastern surface cyclone with a 998 mb central pressure, a deepening of 6 mb over 12 h. As this first low tracks northeast to 32°N, 66°W, the second low, which formed on the surface trough at 13/1800 UTC, tracks northeast to 37°N, 70°W. A third low is analyzed between the two at 33°N, 69°W. Analysis of the position of the third low is based on a 25 kt southeasterly wind from a ship observation northeast of the center. These centers are found in the middle of a larger cyclonic circulation which dominates the analysis area. The coastal trough is associated with the northern-most low center and currently extends from the northern low center to New England. Heavy coastal snow was present with this trough as it moved through coastal New England. The coastal high pressure system has moved east of Nova Scotia and strenghtened somewhat to 1031 mb.

The satellite image (Fig. 10) shows the first low as a weak system in the North Atlantic Ocean. Since the circulation of this low at 32°N, 66°W is very weak, the low clouds west of the center have not wrapped around the low in a typical comma pattern and continue to extend westward. The cloud tops are warmer than indicated in earlier satellite imagery and appear more diffuse in agreement with this initial system. The two new lows which formed on the trough are associated with a mass of organized clouds just east of the mid-Atlantic states. The southern portion of the cloud mass shows two comma clouds forming. The bulge in the clouds at 37°N, 73°W is associated with the new northern low with the frontal structure extending southward. Although most of the second comma structure is masked by higher level clouds, a hook in the southern end of the cloud mass indicates the position of the other center at 33°N, 69°W.

The NMC 850 mb analysis (Fig. 11) merges the three surface centers into one trough centered New Jersey and extending southeast. Dropsondes from the ERICA AWS reconissance flights provided over-water data for this analysis also. The trough extends from northwest to southeast with strong temperature advection in both the cold and warm air. Note the 90° orientation of the isotherms with the height contours. At 700 mb (not shown) a double trough structure lies over the western North Atlantic related to the multiple cyclones. Sixty meter height falls at 700 mb are recorded along the Virginia and Carolina coastlines. Strong warm air advection is evident from 30° to 45°N, 60° to 70°W.

The 500 mb analysis (Fig. 12) shows that the first shortwave, which tracked through the IOP area, has moved east out of the analysis area. From comparisons of the surface center and the 500 mb trough movement, it was found that the upper-level trough moved faster than the first surface cyclone. The trough, at this time, is east of the analyzed surface low position. Development of this initial system has ended. The second 500 mb trough now has reached the coastal waters extending from just west of Wallops Island, Virginia to 25°N, 65°W. Significant height falls of 90 m at Wallops Island and 120 m in North Carolina are observed in the northern portion of the trough. A jet streak of 130 kt at 300 mb (not shown) has propogated through the base of the trough and is located between the two surface systems. The actual position of the jet streak is uncertain due to the scarcity of upper-level observations in that area.

Explosive deepening of the northern center at 37°N, 70°W begins on 14/0000 UTC. By 14/0600 UTC (Fig. 13) the rapidly deepening cyclone is analyzed from ship and buoy data with a central pressure of 980 mb located at 36°N, 66°W. A surface trough extends southeastward to the lower pressures of the first cyclone. A drifting buoy just southeast of the analyzed low position at 14/0600 UTC shows a surface pressure of 983.5 mb giving confidence to the position and central pressure. NOAA P-3 aircraft observations in the area of the low center provided observations from 14/0300 UTC to 14/0600 UTC and also confirm sea-level pressures close to the analyzed values. There is high confidence in the intense deepening rate of 18 mb/ 6 h.

D. 1200 UTC 14 DECEMBER 1988

At 14/1200 UTC the surface analysis (Fig. 14) locates the system at 38°N,64°W with a central pressure of 968 mb. This reveals a 12 h deepening rate is 30 mb per 12 h. The satellite image (not shown) shows a well-developed storm. The 850 mb analysis (not shown) indicates a closed low with strong temperature advection. This system has de-

veloped a closed circulation up through 500 mb (not shown). Strong warm air advection is located northeast of the storm center. The system has rapidly occluded with the 500 mb, 850 mb, and surface centers coincident.

In summary, the IOP-2 event contained several cyclone events. The first center of the IOP-2 cyclone development formed east of Florida. This low developed in response to a first 500 mb shortwave trough as it approached the southeast U.S. coastline. As the trough moved east of the surface low, the storm stopped developing and deepened only to 998 mb at 14/0000 UTC. A surface trough had developed at 13/1200 UTC from the initial low extending north-northwestward to New England. Two lows formed on this trough in response to intense upper-level forcing as a second 500 mb trough, which was much stronger, reached the coast. The northernmost cyclone in the 14/0000 UTC analysis is the cyclone that rapidly deepens. By 14/1200 UTC, this cyclone experienced central pressure falls of 30 mb in 12 h, dropping to 968 mb. This was truly a case of concentrated rapid cyclogenesis observed by the ERICA project. Model performance in forecasting the rapid cyclogenesis is discussed in the next chapter.

IV. PROGNOSTIC MODEL DISCUSSION

A verification of NMC NGM and Spectral Model forecasts of the IOP-2 event was conducted. The objective was to determine if the operational models were able to forecast the rapid cyclogenesis, the correct movement of the cyclone, and the multiple centers. To accomplish this, all available model forecasts and analyses were compared to the subjective surface analyses and the NMC 500 mb analyses.

The 12-h to 48-h model runs verifying at 13/1200 UTC show the initial surface cyclone moving too slow compared to the subjective analysis. For the longer forecast periods, the center is forecast northwest of the analyzed storm position. Each succeeding forecast valid for 13/1200 GMT accelerates the movement of the cyclone so that the final objective analysis position at 00 h is northeast of the subjective analysis position (Fig. 2). The average central pressure of the forecast cyclones is 1-2 mb higher than both the subjective analysis and the NGM objective analysis. At 500 mb the vorticity center associated with the surface low on all forecasts also lags the actual eastward movement of the observed vorticity center. The forecast intensity of the second trough moving through the midwest is too weak at 48 h and 36 h, but improves on the 24-h and 12-h forecasts. The NGM also places this trough too far west on the 48-h and 36-h forecasts, which is then corrected on subsequent 24- and 12-h forecasts, where both position and intensity are generally good. In general, the vorticity maxima associated with both troughs on the 500 mb NGM forecasts are forecast too slow.

The Spectral Model was also available on 13/1200 UTC with the 12- and 24-h forecasts and 00-h analysis. The forecast cyclones are slightly north of the observed cyclone for all forecasts. The central pressures of the forecast cyclones are within $\pm$ 2*mb* of the observed pressure. At 500 mb the NGM objective analysis was used for verification as the Spectral Analysis was unavailable. The overall 500 mb forecasts of the two vorticity maxima associated with the shortwave troughs were successful. However, there are minor deficiencies. The 24-h position forecast for the first shortwave was better than the too-slow 12-h forecast. For the second shortwave, the 12-h forecast is quite accurate, but the 24-h forecast is slow and somewhat weak.

At 14/0000 UTC the NGM model fails at all forecast times to predict three centers, although the two 500 mb shortwave troughs approaching the ERICA region were forecast correctly. The model only hints at the observed surface trough which stretches

northward to Massachusetts by extending the low pressure area northeastward. The model overdeepens the single low especially at the 24-h and 12-h forecast periods as compared to any of the three lows, which all have 998 mb central pressure. The 24-h forecast shows a central pressure of 990 mb while the analysis indicates a higher central pressure of 998 mb with multiple centers. The 36-h NGM single low forecast is close to the position of the first cyclone at 32°N, 66°W. This suggests that the model was unable to predict the observed smaller scale surface evolution. The NGM storm center position is shifted farther north and west with each successive forecast. Even the NGM objective analysis (00-h) resolves only one low near the midpoint position of the three observed cyclones clearly indicating the inability of the model to resolve separate smaller scale features. A summary of the cyclone position and central pressure error is listed in Table 1. At 500 mb, the 36-h forecast verifying at 14/0000 UTC erroneously indicates that the two vorticity maxima are close to each other. The vorticity maximum associated with the first shortwave is east of the low analyzed by the NGM. The PVA associated with the second shortwave trough is just west of the low center providing upper-level support for cyclogenesis of this surface low, which was the eastern, non-developing low determined by the analysis. The 12-h and 24-h forecasts merge the two vorticity maximums into one area, which is not representative of the two separate and distinct analyzed shortwave troughs that moved through the ERICA region and produce rapid development of the northern center.

The 12-h, 24-h, and 36-h Spectral Model forecasts for 14/0000 UTC were also available. Similar to the NGM, the Spectral also missed the formation of the center which formed on the trough just east of the mid-Atlantic coastline. The 24-h forecast indicates more of this trough than the other time periods, although it is still recognizable on the 12-h and 36-h forecasts. The Spectral forecast central pressure is 8 mb deeper on average than the observed pressure of 998 mb, while the position of the model's single forecast cyclone at all time periods is in the vicinity of the average position of the three cyclones observed at this time. Table 1 lists the surface position and central pressure errors of the Spectral Model also. The Spectral Model forecast two 500 mb vorticity maxima at 36 h and 24 h. Like the NGM, the Spectral Model forecasts valid at 14/0000 UTC show one vorticity maximum east of the forecast and observed cyclone positions. The second vorticity center associated with the shortwave trough is west of the forecast surface low center. Figure 15 shows the positive vorticity advection from this vorticity maximum is just west of the model's cyclone position. This forecast PVA is especially significant north of the low in the forecast and is in the area where PVA would provide

upper-level forcing for the low at 37°N, 70°W, which rapidly deepened but was not forecast by the model.

Both models fail at all forecast periods to forecast the multiple cyclones which were observed at 14/0000 UTC. The position of the single cyclone predicted by the models is an average position in the vicinity of the three observed cyclones. The 500 mb shortwaves position and intensity were forecast accurately in both models with an error in only two forecasts, the 12- and 24-h NGM forecasts, where the two vorticity maxima associated with each trough were combined. The error was corrected at shorter forecast time periods due to better initial analyses.

Table 1. IOP-2 FORECAST SUMMARY: 14/0000 UTC

Model	Surface Position Valid 14/0000 UTC	Surface Intensity Valid 14/0000 UTC	Error (forecast - observed)
Analysis	37°N,70°W 33°N, 69°W 32°N, 66°W	998 mb	
Nested Grid Model			
36 h	34°N, 69°W	000 mb	2 mb
24 h	35°N, 70°W	990 mb	-8 mb
12 h	34°N, 67°W	993 mb	-5 mb
00 h	36°N, 69°W	996 mb	-2 mb
Spectral Model			
36 h	35°N, 67°W	988 mb	-10 mb
24 h	35°N, 67°W	989 mb	-9 mb
12 h	35°N, 68°W	991 mb	-7 mb

At 14/1200 UTC one low is shown on both the NGM forecasts and the analysis. The NGM forecasts and the subjective analysis of the cyclone are in good agreement, in positioning the rapidly deepening cyclone. The 48-h forecast underdeepens the storm with an error of 16 mb. The 12-h forecast has a central pressure of 967 mb which is only 1 mb lower than the observed central pressure. The operational NGM analysis increases the central pressure to 973 mb which is 5 mb higher than observed. Surface pressure and forecast positions are summarized in Table 2. All 500 mb forecasts indicate one vorticity

maxima at 14/1200 UTC east of the forecast surface cyclone center. The forecast PVA is located northeast of the cyclone center along the track of the observed explosive cyclone.

For 14/1200 UTC the Spectral Model 24-, 36-, and 48-h forecasts also had good placement of a single rapidly deepening cyclone, but the model underdeepens the forecasted low in the 24-h forecast by 4 mb. The forecast central pressure of the low is 964 mb on the 48-h forecast whereas the subjective analysis indicates a 968 mb central pressure. This is true in spite of incorrectly forecasting the evolution at the surface. Subsequent forecasts produced a higher cyclone central pressure. A summary of position and central pressure forecasts are presented in Table 2 for forecasts valid 14/1200 UTC. At 500 mb, the trough placement in the 48-h and subsequent forecasts correctly predicts the vertical structure of the system with respect to the surface center.

Table 2. IOP-2 FORECAST SUMMARY: 14/1200 UTC

Model	Surface Position Valid 14/1200 UTC	Surface Intensity Valid 14/1200 UTC	Error (forecast - observed)
Analysis	38.5°N, 64°W	968 mb	
Nested Grid Model			
48 h	38°N, 65°W	984 mb	16 mb
36 h	38°N, 67°W	974 mb	6 mb
24 h	38°N, 63°W	975 mb	7 mb
12 h	39°N, 65°W	967 mb	-1 mb
00 h	39°N, 64°W	973 mb	5 mb
Spectral Model			
48 h	39°N, 65°W	964 mb	-4 mb
36 h	39°N, 64°W	968 mb	0 mb
24 h	39°N, 63°W	971 mb	3 mb

In IOP-2, both the NGM and Spectral Prognostic Models were unable to forecast the multiple lows which developed at 14/0000 UTC. The forecasts from both models indicates one low forming just east of Florida and rapidly deepening as it tracked northeastward. The NGM forecast the single cyclone in the average position of the

multiple lows at 14/0000 UTC and overdeepened the low for longer forecast periods. The Spectral model also overdeveloped the single cyclone for all forecasts. By 14/1200 UTC the position of the cyclone forecast by both models agrees well with the analysis. At this time, the NGM and Spectral Models generally underdeepen the low. The maximum NMC surface forecast error of IOP-2 was in the NGM 48-h forecast where the forecast was 16 mb too high. Both models' forecasts indicate rapid deepening, but the cyclone forecast by the model to intensify apparently was not the northern cyclone that was observed to explosively deepen. The 500 mb forecast of trough positions and positive vorticity advection were relatively accurate. The models were able to forecast the upper-level features reasonably well even though the surface forecasts were poor.

V. DIAGNOSTICS OF IOP-2 CYCLONE

A hypothesis used in previous studies to explain rapid cyclogenesis is that rapid development of marine cyclogenesis represents a favorable superposition of upper- and lower-level forcing mechanisms under low static stability conditions. By looking at each of the requirements separately, the applicability of this hypothesis to IOP-2 will be evaluated. The dynamics of IOP-2 cyclone are also considered using the Omega equation. The operational NMC Spectral Model analysis gridpoint data are used to study the upper- and lower-level forcing and the static stability of the cyclone throughout the rapid cyclogenesis stage of development. Although the Spectral Model forecasts had some errors in forecasting the rapidly deepening cyclone, consideration of the dynamics initially using the model data is helpful to provide insight into the explosive cyclogenesis problem.

The Omega equation is a diagnostic equation used in the mid-latitudes to estimate the vertical velocity, an important measure of cyclone development (Holton, 1979). The equation (Eqn. 1) is derived from the vorticity and thermodynamic equations following the Quasi-Geostrophic assumptions. The key assumption of Quasi-Geostrophic theory is that the atmosphere has a strong tendency to maintain geostrophic and hydrostatic balance. The vorticity and thermodynamic equations have two independent variables, omega (ω) and geopotential height (ϕ). Together the vorticity and the thermodynamic equations form a closed set of equations from which the Omega equation is formed by eliminating $\frac{\hat{c}\phi}{\hat{c}t}$ between the two equations. The Omega Equation estimates vertical velocity from differential vorticity advection, the Laplacian of thermal advection, diabatic heating, and frictional forcing, as follows:

$$[\nabla^2 + \frac{f_0}{\sigma}\frac{\hat{c}^2}{\hat{c}p^2}]\omega = \frac{f_0}{\sigma}\frac{\partial}{\hat{c}p}[V_g \cdot \nabla[\frac{\nabla^2\phi}{f_0} + f]] + \frac{1}{\sigma}\nabla^2[V_g \cdot \nabla[-\frac{\hat{c}\phi}{\hat{c}p}]]$$

$$-\frac{1}{\sigma}\nabla^2[\frac{R}{C_p}\frac{Q}{p}] - \frac{f_0}{\sigma}\frac{\hat{c}}{\hat{c}p}(k \cdot \nabla \times F) \qquad (1)$$

Upward vertical velocity over the cyclone center is a necessary condition for cyclone development. Thermal advection is due to the circular airflow around the cyclone located on a frontal zone. Over the cyclone center the thermal advection is small, so that upward vertical motion must be produced by differential vorticity advection rather than by thermal advection. Vorticity is a maximum in the trough and an minimum in the ridge, and, generally, the maximum positive vorticity advection occurs between the trough and the ridge over the surface center. Vorticity advection is small at the surface because of the nearly circular flow. Therefore, differential cyclonic vorticity advection can be approximated by the upper-level PVA. PVA in this discussion is determined from the Spectral Model grid point data at 500 mb.

Localized warm advection or positive thickness advection produces upward vertical motion aiding the development and movement of the cyclone. Localized diabatic heating is also a cause of upward vertical motion due to the latent heat released. The frictional term is a maximum within the boundary layer. It will indicate upward motion for cyclonic circulations due to boundary layer convergence.

All terms considered together will estimate the magnitude of upward vertical motion from the horizontal temperature and height fields. The Omega equation terms are multiplied by the factor $\frac{1}{\sigma}$, where σ is static stability. Since the static stability term is in the denominator throughout the equation, a decrease in static stability will increase the vertical motion forced by each term.

The static stability parameter is estimated in this study by the temperature difference between 500 mb and 1000 mb divided by the pressure interval, $SI = [\frac{\theta_{500} - \theta_{1000}}{500mb}]$. The static stability values decrease if θ_{500} decreases or θ_{1000} increases. If a parcel is lifted dry adiabatically from the surface and is cooler than the upper-level environmental temperature, the system is stable and the static stability parameter will have high positive values. The effect of high values of static stability is to impede the upward vertical motion, which significantly alters the development of the cyclone. Low static stability provides a more efficient environment for forcing vertical motion.

Since errors in numerical products would produce erroneous results in analysis, the surface isotherm pattern from the gridded data was compared to a subjective surface temperature analysis from observations including drifting buoy data. In general, the numerical fields were close to the observations with some departures due to smooth gridpoint fields. The maximum differences averaged a few degrees with the numerical analyses showing slightly warmer 1000 mb temperatures over the western North Atlantic Ocean than the subjective analysis. Wind fields for both the subjective analysis and the

model were not compared, although the errors due to a poor model analysis may significantly alter thermal advection.

This section will focus on three key time periods of the ERICA IOP-2 storm, 13/1200 UTC, 14/0000 UTC, and 14/1200 UTC. At 13/1200 UTC the subjective analysis (Fig. 2) places the cyclone at 28°N, 72.5°W with a central pressure of 1004 mb while the gridded data locates the cyclone at 32°N, 73°W. The 1000 - 500 mb thickness pattern shows a more enhanced 'S' shape in the vicinity of the cyclone and a broad closed isobar around the cyclone (Fig. 16). This seems to suggest greater amplitude of the thermal wave than in the subjective analysis.

At 850 mb (Fig. 17) the 1,420 m contour is almost closed over the surface low, which is accurate compared to the 850 mb analysis (Fig. 4). Warm air advection is present on the eastern portion of the trough and is centered on a line from 27°N, 65°W to New Jersey and then extends northward through New England. The warm air advection is just east of the sea-level low pressure system. At the same level, the cold air advection is southwest of the 850 mb trough line. The cold advection is from 75°W to 85°W and over Florida and southern Georgia. At 700 mb (not shown) significant warm air advection is downstream of the trough axis. East of the low center and centered on 32°N, 66°W, the warm air advection maximum is $+18 \times 10^{-5}$°C/ sec . West of the sea-level low center, the thermal advection is weak. The strongest cold air advection is west of the second trough with -18×10^{-5}°C/ sec over Mississippi. The thermal advection patterns at both 850 mb and 700 mb indicates upward vertical motion from the Omega Equation east of the sea-level low supporting development of the first cyclone center.

The 500 mb positive vorticity advection (Fig. 18) indicates two maxima, one associated with each of the two shortwave troughs. The first shortwave PVA maximum is northeast of the surface cyclone 28°N, 72.5°W in the subjective analysis. This weak PVA maximum is east of the sea-level low pressure area. The PVA east of the sea-level low is due to the more rapid eastward propogation of the upper-level trough than the surface cyclone, which is evidence of the weak coupling between the lower and upper troposphere. Recall that this first cyclone starts to weaken after this time and deepened only 2 mb in the next 12 hours ending at 14/0000 UTC. The second PVA maximum is stronger and centered on 37°N, 79°W. The surface trough (Fig. 2) forms off the Virginia coastline in response to the upper-level forcing by this shortwave trough. At 13/1200 UTC the static stability (Fig. 19) east of the southeastern U.S. lowers to 20K/500 mb in an enclosed area centered on 28°N, 74°W roughly over the surface cyclone and trough and in an area of localized low-level warm air advection at 700 and 850 mb. Static sta-

bility is higher over the initial cyclone to the east contributing to the decoupling of the surface system with the upper-level flow and slower development.

The surface gridded data at 14/0000 UTC (Fig. 20) shows an increasing amplitude in the thickness pattern from the last 12 hours. The objective analysis indicates one low, which is inconsistant with the observed number of cyclones in the subjective analysis. The location of the low suggested by the thickness pattern, is at 34°N, 67°W. This position is in the vicinity of the three observed cyclones, but does not resolve the individual lows.

At 700 mb (Fig. 21, 850 mb is not available) the localized warm air advection maximum of $+32 \times 10^{-5}$°C/ sec is centered at 35°N, 60°W. This position is upstream of the 700 mb trough axis and east of all the observed surface lows. Weak localized warm air advection of $+8 \times 10^{-5}$°C/ sec extends northwestward to Massachusetts. Cold air advection is found west of the trough line from the southeastern U.S. to 73°W. Although the gridded data shows only one sea-level low pressure system and an increase in the thickness advection, the weak thermal advection pattern near the western low still supports future development. Upward vertical motion in the Omega equation is indicated from the localized advection of warm air, although it is weak over the western center, which rapidly deepened. Part of the lack of the thermal advection over the western low may be due to the inability of the gridded anlaysis to resolve the smaller scale details at 850 and 700 mb.

The 500 mb PVA (Fig. 22), associated with the second shortwave trough, is a maximum of $+ 2.4 \times 10^{-9} s^{-1}$ is located at 37°N, 69°W. This PVA maximum is almost directly over the northernmost cyclone analyzed at 14/0000 UTC. This strong PVA signature is evidence of the strong upper-level forcing associated with the second upper-level trough. This PVA center is significantly north of the first cyclone.

The low static stability center of 15°K/500 mb at 14/0000 UTC (Fig. 23) is located at 35°N, 73°W in an area of weak surface warming, but the significant warming is located northeast of that minimum static stability area. Surface warming was determined by the temperature change over the 12 h ending at 14/0000 UTC from the Spectral Analyses. Surface temperature changes (Fig. 24) are calculated at each gridpoint for the 12 h period ending 14/0000 UTC. Surface warming is centered on 37°N, 64°W roughly in the area of static stability of 18K/500 mb that extends northeast from the minimum of 15K/500 mb. The surface warming indicates low troposphere destabilization along the path of the rapidly deepening cyclone. Maximum cooling at 500 mb (not shown) of 6K is centered on 33°N, 75°W, northwest of the area of lowest static stability, al-

though cooling is present over the low static stability area. The cooling aloft is due to the movement of the upper-level shortwave offshore. The cooling at 500 mb and the warming at 1000 mb are responsible for the decrease in the low static stability values analyzed in the 14/0000 UTC data. The lowering of the static stability creates an environment conducive to the rapid cyclogenesis which occurs over the suceeding 12 h. The operational analysis may underestimate the static stability due to the tendency of the objective analyses to be warmer than observed, but the thermal advection at low levels is also poorly known.

By 14/1200 UTC explosive development has occurred and one low dominates the synoptic pattern and the subjective analysis including drifting bouy and ship data places the surface cyclone center at 38.5°N, 64°W (Fig. 14) with a central pressure of 972 mb. The Spectral Model analyses also indicate a single low at 38°N, 64°W (Fig. 25). Lower thickness values are found on the southwestern quadrant of the cyclone, while greater thickness values are east and north of the cyclone center showing the intense amplification of the system. At 850 mb (Fig. 26), the cold air advection is south of the cyclone. The strong warm air advection at 850 mb $+36 \times 10^{-5}$°C/ sec , is east and north of the cyclone center, as it is at 700 mb as well. The cold air advection has wrapped around the low center and is southeast of the cyclone at 700 mb. The 500 mb cyclonic vorticity advection (Fig. 27) is weaker than 12 hours previously with the center located at 42°N, 60°W. An equally intense maximum of negative vorticity advection is present southwest of the cyclone center.

By 14/1200 UTC the static stability (Fig. 28) minimum is analyzed in the gridded data to rise to 18K/500 mb. The increase in stability in the layer appears to be due to cooling at 1000 mb. The static stability minimum is in an area where the 12-h temperature difference indicates cooling of 6K and is southwest of the storm center. At 500 mb, the cooling is as strong as 12 h previously (6K) and is located directly over the area of lowest static stability. The cooling at 500 mb would favor a lower static stability. Instead of warming at 1000 mb, the 12-h trend is for cooling at the surface as cold air surges eastward behind the cold front. This leads to a slight increase in stability for this time period.

Since that upward vertical motion is instrumental in promoting development of the cyclone, its consideration is especially interesting in the case of the multiple lows that developed in IOP-2. The first cyclone developed when both thermal advection and PVA associated with the first shortwave were in phase. As the first shortwave trough moved east of the surface cyclone, the upward vertical velocity was weakened and the cyclone

filled. The gridded data indicates the first cyclone lost the upper-level support, while the rapidly deepening cyclone, which formed on the surface trough, located at 37°N, 70°W, intensified due to the influence of the second, stronger shortwave trough. The second shortwave trough produced PVA, north of the initial surface low. The explosive low developed in an area of weak localized warm air advection based on the Spectral Model analyses and it may have been stronger, low static stability, and strong PVA north of the original cyclone.

Considering the hypothesis on rapid cyclogenesis, these results show clear evidence of upper-level forcing in the region of the rapidly deepening cyclone. Also the static stability lowered to a minimum value at 14/0000 UTC. Wash et al. (1988) indicates that the static stability of rapidly deepening storms decreases during the first 60 h of the storms development. The destabilization of the 1000 to 500 mb layer occurred due to warming at the surface. The rapidly deepening cyclone in IOP-2 was also associated with a decrease in the static stability in the development region and along the storm track. Although the lower-level forcing shown by the localized warm air advection was weak, it remains to be accurately assessed in future detailed low-level analyses. Since the grid point analyses are from operational data, most ERICA data will not be reflected in these analyses. Consequently, these low-tropospheric thermal and wind analyses may not be representative of the true conditions. Still, considering this as a first-look at IOP-2, these results show that localized warm air advection may not have been a significant factor in the rapid cyclogenesis for this case.

The rapid cyclogenesis analyzed in IOP-2 indicates that only two of the four requirements of the hypothesis for rapid cyclogenesis were present. The rapidly deepening cyclone developed in response to strong positive vorticity advection associated with a 500 mb shortwave though. The static stability was low in the area of the cyclone development due to surface warming and 500 mb cooling. Missing were a pre-existing surface disturbance and low-level forcing. The maximum localized warm air advection was well to the east of the explosive cyclone. The results of the study of IOP-2 suggest the hypothesis may need to be revised.

VI. CONCLUSIONS AND RECOMMENDATIONS

The ERICA IOP-2 cyclone was especially difficult to forecast due to the numerous surface low pressure systems that developed during the observation period. The first low developed east of Florida as a short wave trough at 500 mb moved over the southeastern U.S. and the western North Atlantic Ocean. This low did not rapidly deepen, but a surface trough did form extending from the low to New England. The rapidly deepening cyclone formed on the surface trough as a second, stronger shortwave trough at 500 mb moved offshore. The rapidly deepening low deepened at the rate of over 30 mb for the 12 h ending at 14/1200 UTC.

Data collected during IOP-2 proved essential in the study of this storm. Drifting buoy, ship, and aircraft data pinpointed the three lows at 14/0000 UTC. Subjective analyses were in agreement with satellite imagery which showed circulation in the enhanced clouds and two comma patterns at 14/0000 UTC related to the multiple lows.

The numerical models, the NGM and Spectral Model, developed only one low instead of the multiple lows observed. The models predicted the one cyclone to track northeastward while it rapidly deepened. The NGM did not predict central pressures as low as those that were observed. At 14/1200 UTC, the NGM 48-h forecast indicated the central pressure 16 mb too high, which is the worst example of model failure in forecasting central pressure for this case. Other deficiencies existed as well. The Spectral model also developed only one surface cyclone and overdeepened the initial cyclone with a northeastward track. The 500 mb forecasts from both models show the vorticity maxima associated with each shortwave trough observed during IOP-2. At longer forecast periods the NGM combined the vorticity maximums into one extended area, which was not representative of the two shortwave troughs that passed through the ERICA region. In general, the NMC 500 mb forecasts accurately depicted the upper-level features.

The reasons for the cyclone development were investigated following quasi-geostrophic diagnostics. The Omega equation forcing terms were analyzed for IOP-2 using the NMC operational Spectral Model analysis gridpoint data. Positive vorticity advection was found in the region of the rapidly deepening storm. Upward vertical motion was likely enhanced by low static stability due to surface warming and 500 mb cooling. The hypothesis used for many studies into rapid cyclogenesis is that a pre-

existing cyclone, upper- and lower-level forcing, and low static stability are required to occur simultaneously for rapid cyclogenesis to occur. In IOP-2 only upper-level forcing and low static stability were prominent in the gridded analyses. The low-level forcing was well to the east of the cyclogenesis area and the cyclone formed in response to a strong 500 mb shortwave trough rather than from superposition with a pre-existing surface center. Key questions remain about the low-level forcing due to deficiencies in the model analyses of the multiple centers.

Recommendations for future study include looking at additional ERICA data available later this year. First, aircraft dropsondes will provide more detail on the stability patterns and low-level forcing and should be incorporated into the IOP-2 study. Second, satellite soundings for key ERICA periods should be studied to measure the static stability and other important features of ERICA cyclones. Finally, IOP-2 is only one of several interesting cases in ERICA that need to be analyzed. Although IOP-2 suggests modification of the hypothesis on the physical processes leading to rapid cyclogenesis, the study of other ERICA cyclones will provide additional insight into the processes responsible for rapid cyclogenesis.

APPENDIX A. FIGURES ILLUSTRATING THE EVENTS OF IOP-2

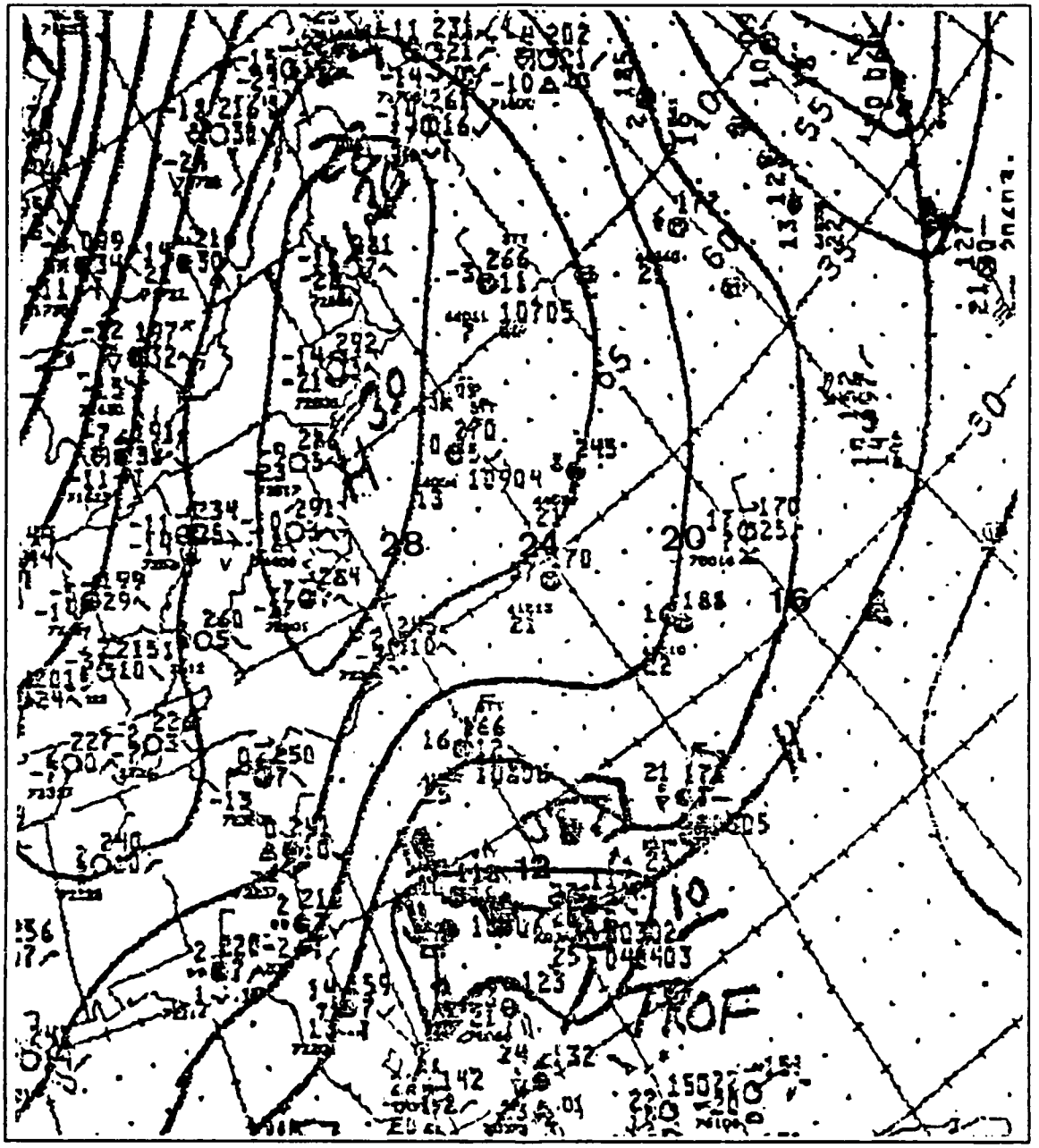

Figure 1. NMC MSLP analysis for 13/0000 UTC December 1988.

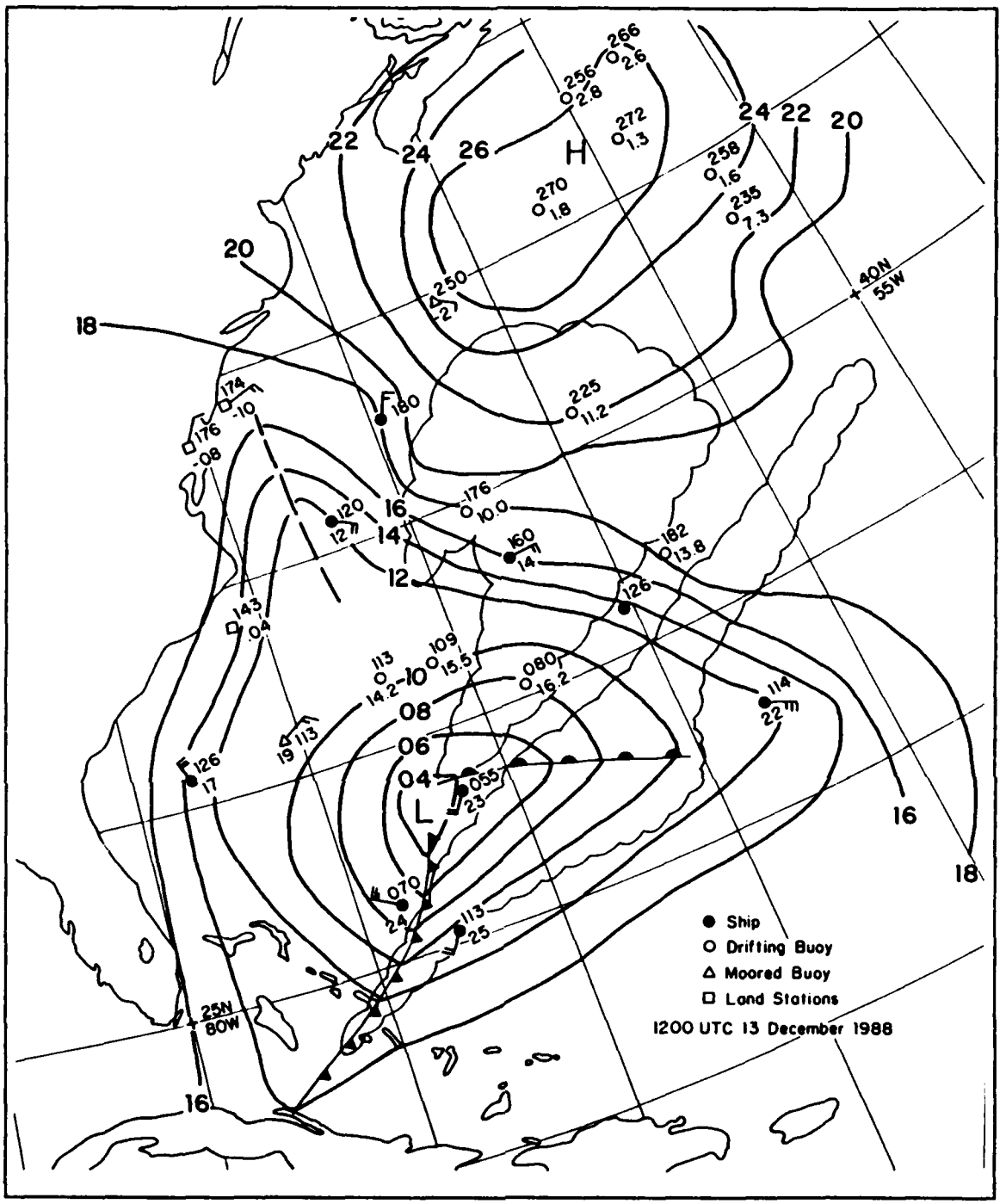

Figure 2. Subjective MSLP analysis for 13/1200 UTC December 1988. See legend for data types. Major cloud areas indicated from GOES imagery.

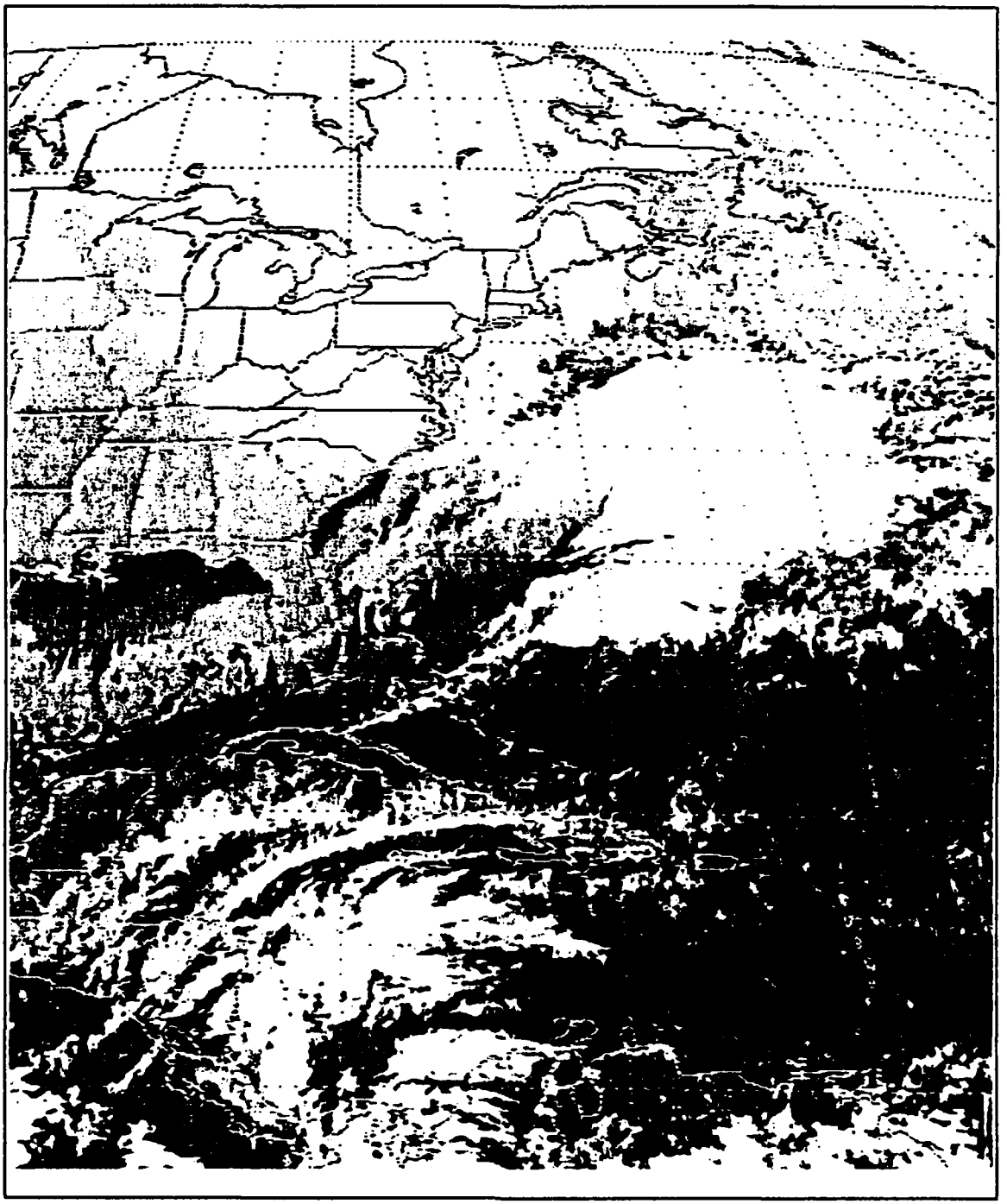

Figure 3. Goes infrared east coast U.S. sector imagery for 13/1200 UTC December 1988.

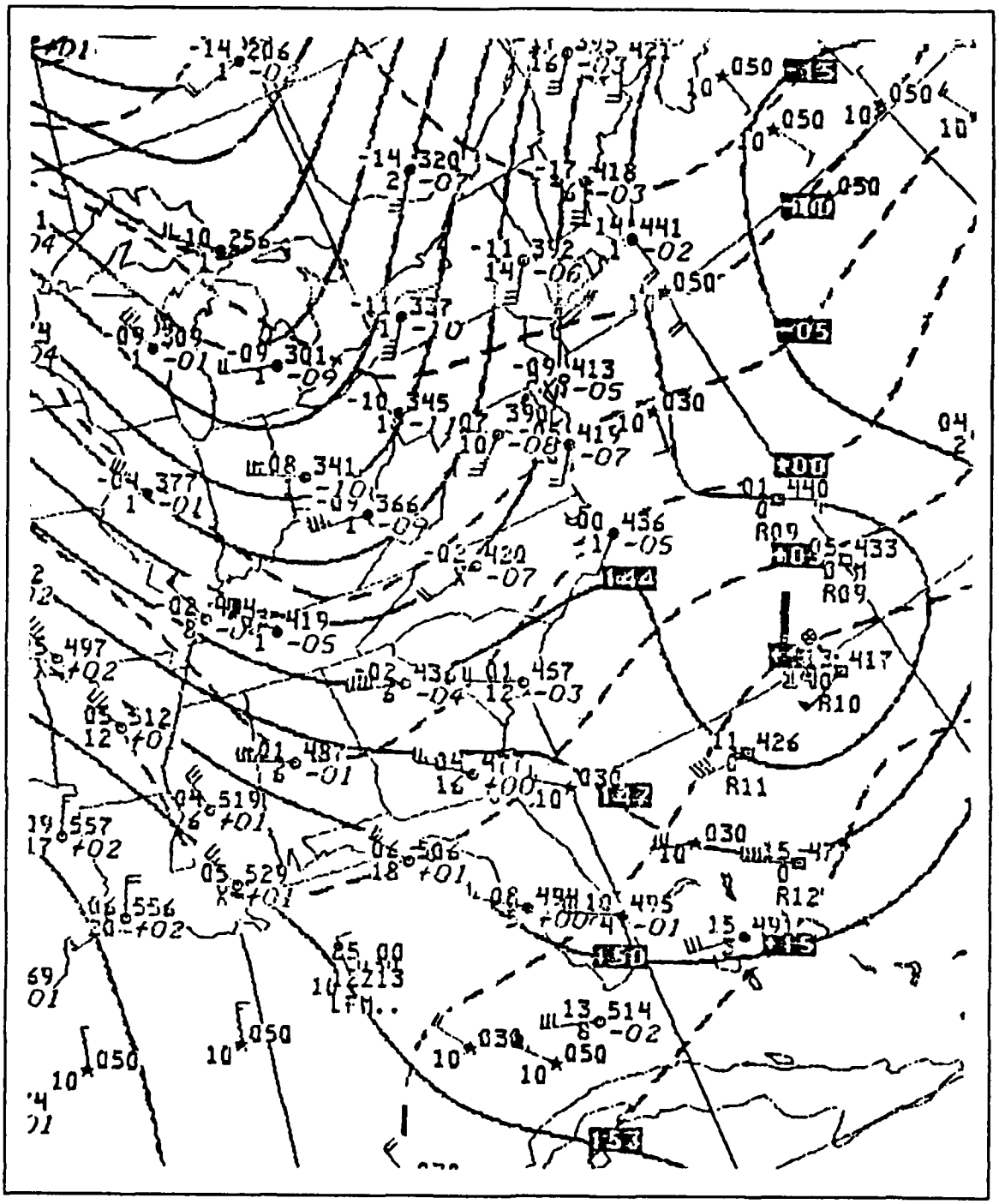

Figure 4. NMC LFM operational 850 mb analysis for 13/1200 UTC with geopotential height (m, solid) and isotherms (°C, dashed).

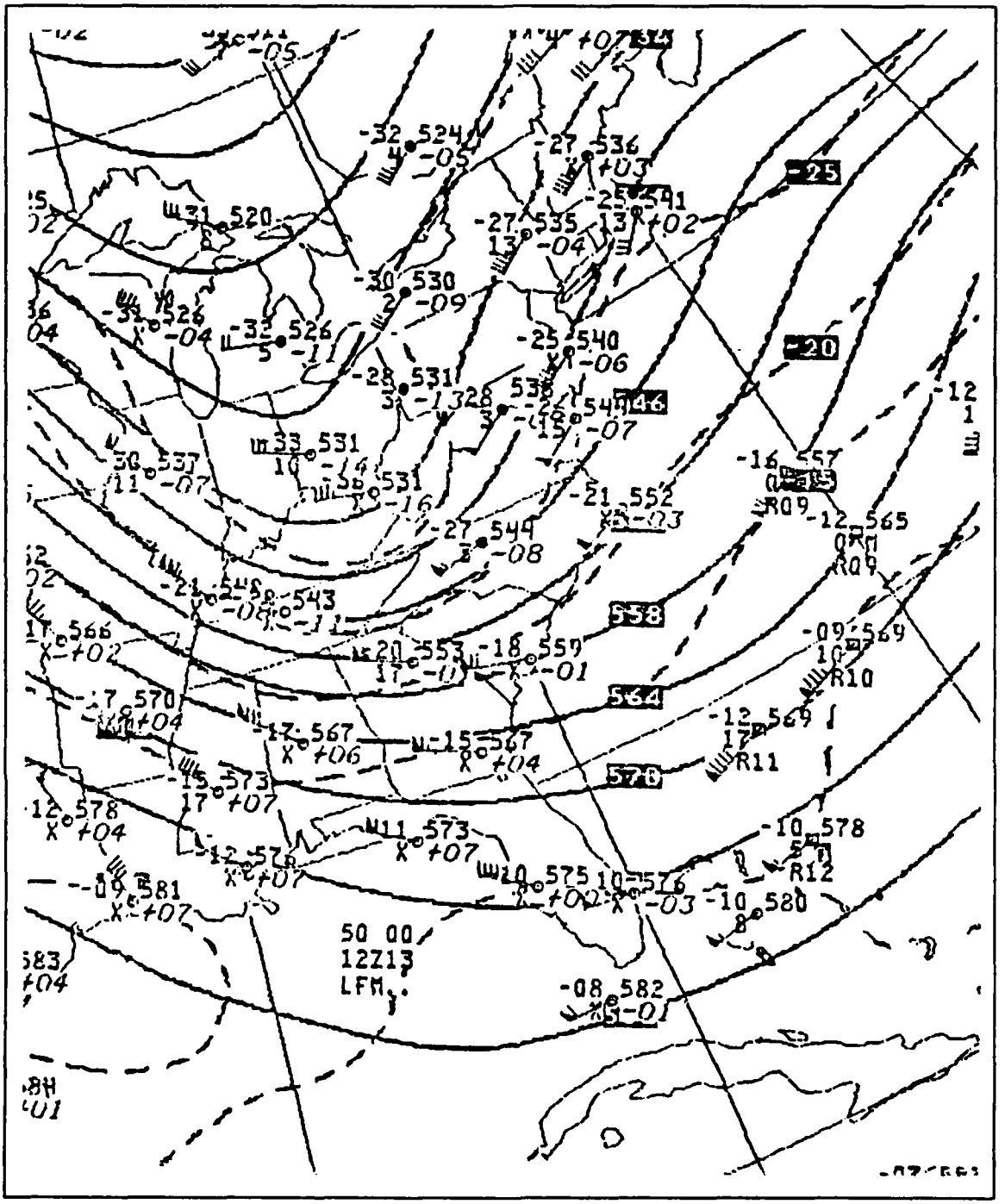

Figure 5. NMC LFM operational 500 mb analysis for 13/1200 UTC with geopotential height fields (m, solid) and isotherms (°C, dashed).

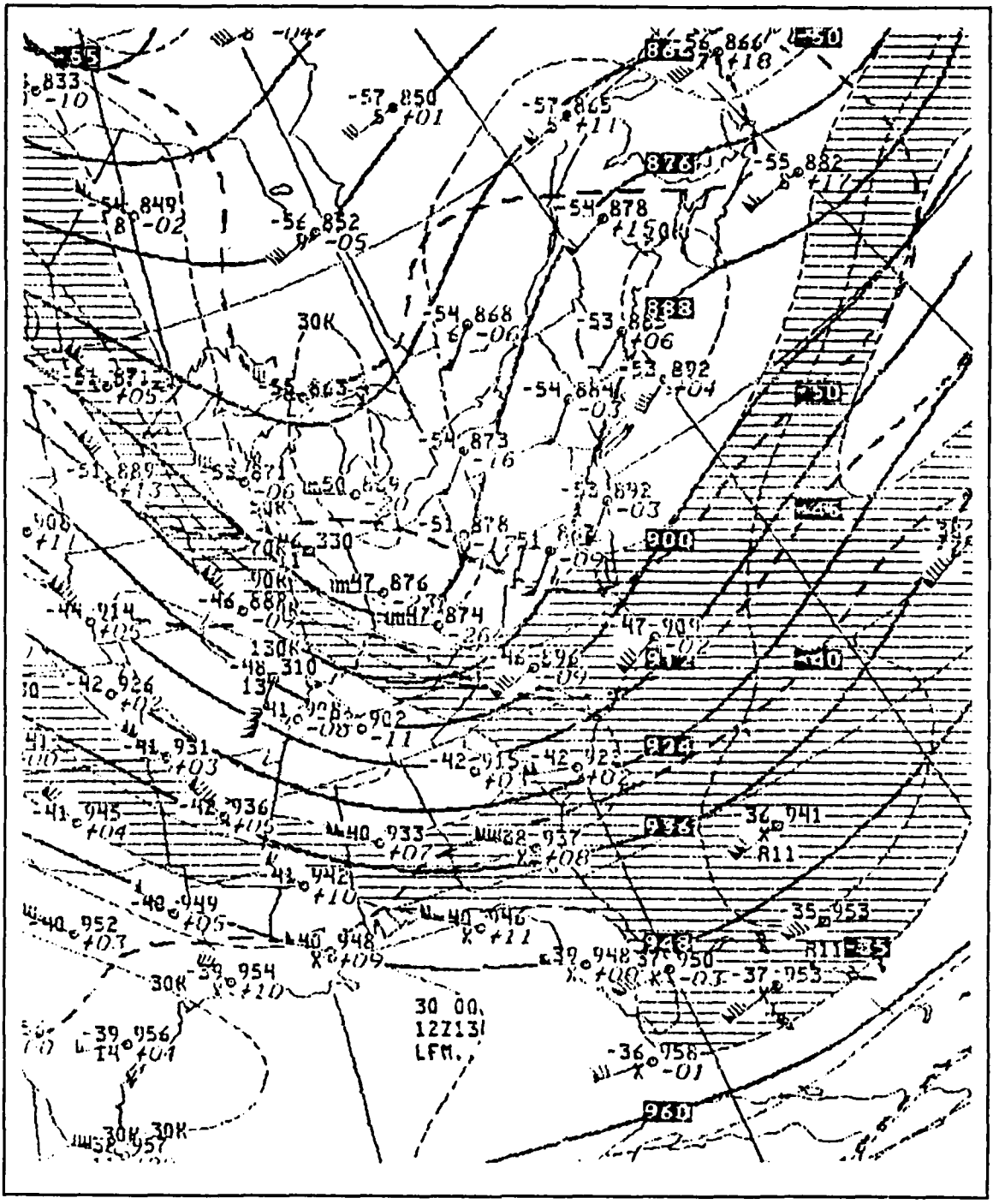

Figure 6. NMC LFM operational 300 mb analysis for 13/1200 UTC with geopotential height (m, solid) and isotach (kt, dashed). Wind fields above 90 kt are shaded.

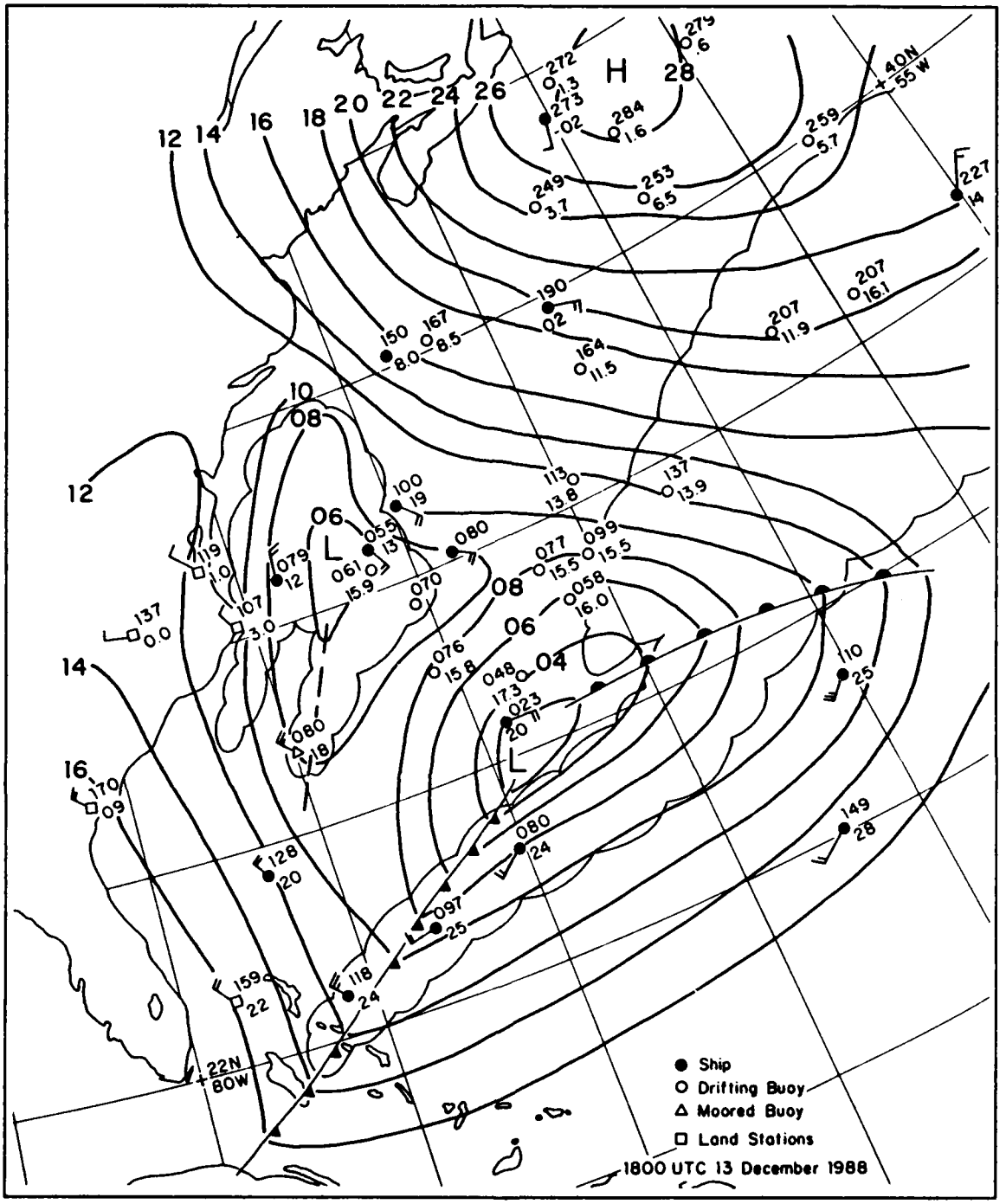

Figure 7. As in Figure 2 except for 13/1800 UTC December 1988.

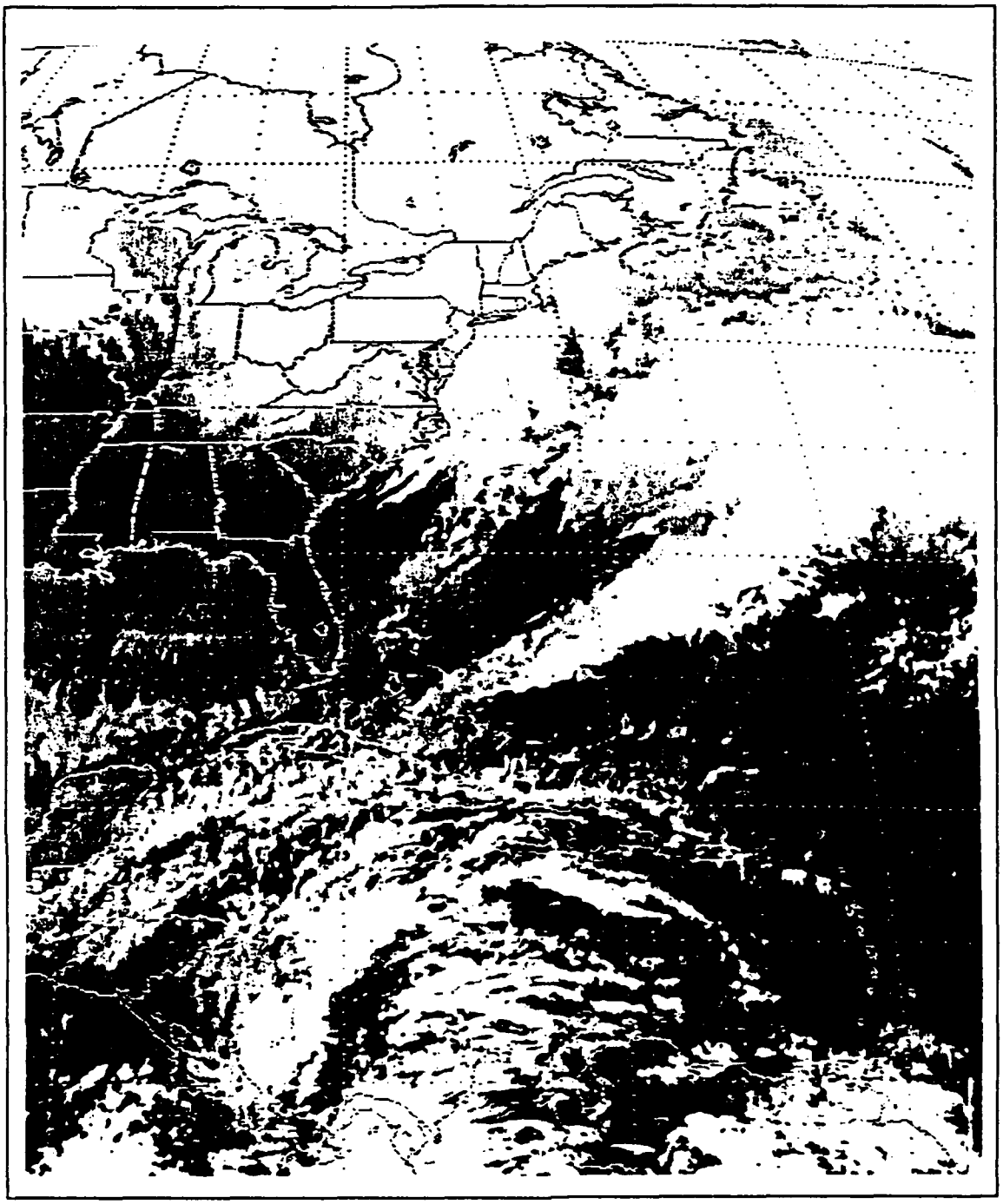

Figure 8. As in Figure 3 except for 13/1800 UTC December 1988.

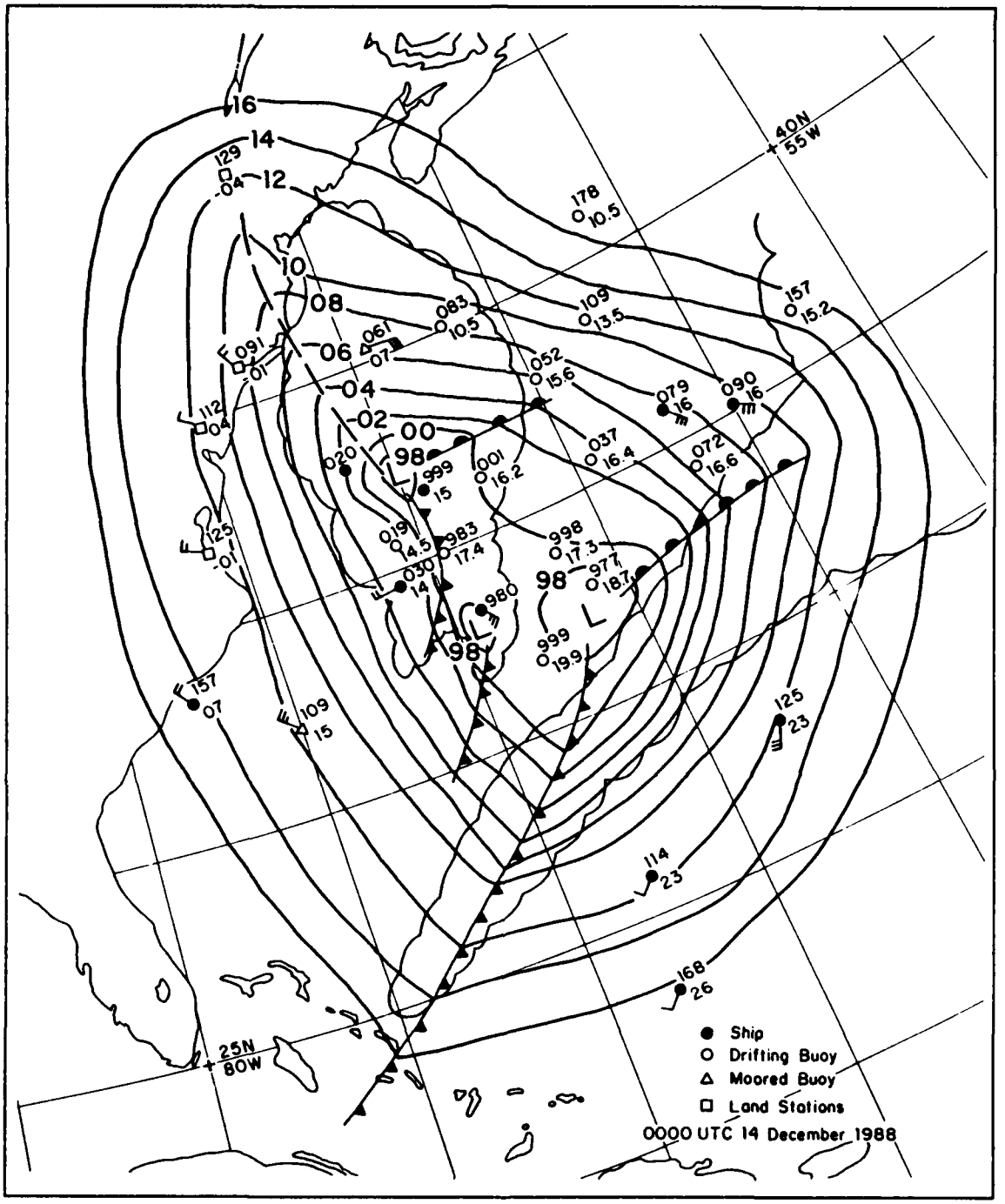

Figure 9. As in Figure 2 except for 14/0000 UTC December 1988.

Figure 10. As in Figure 3 except for 14/0000 UTC December 1988.

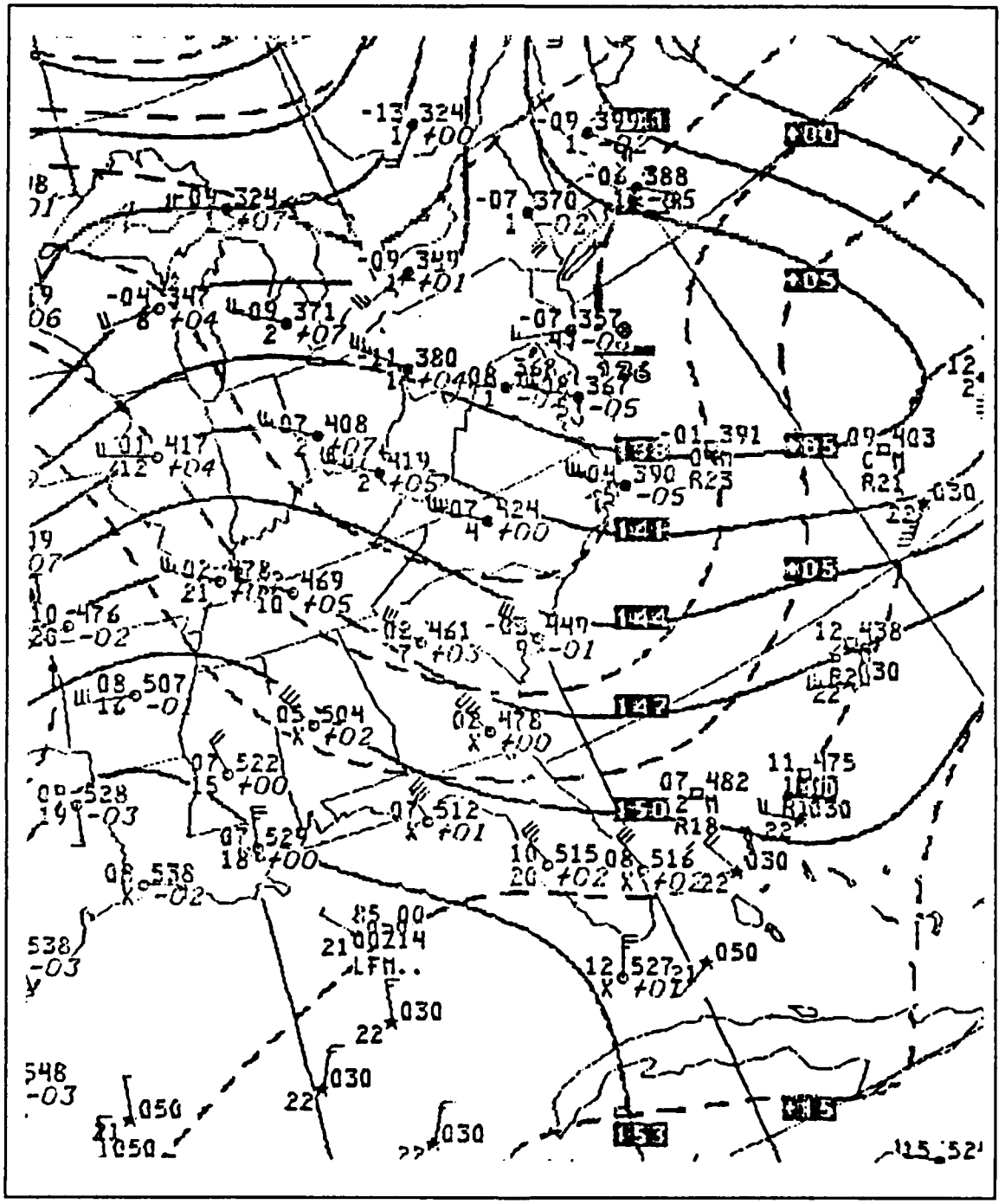

Figure 11. NMC LFM operational 850 mb analysis for 14/0000 UTC with geopotential height (m,solid) and isotherms (°C, dashed).

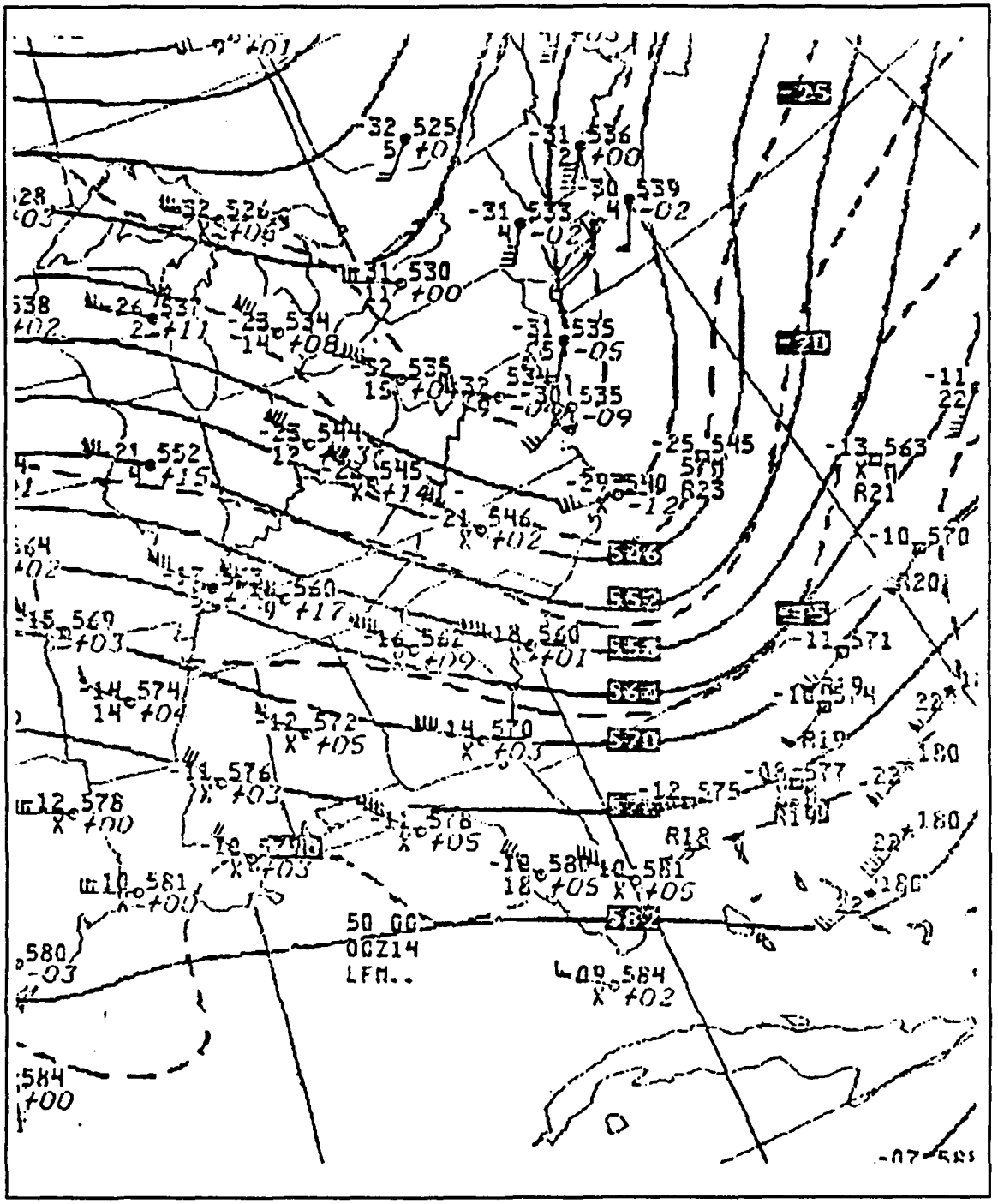

Figure 12. NMC LFM operational 500 mb analysis for 14/0000 UTC December 1988 with geopotential height (m, solid) and isotherms (°C, dashed).

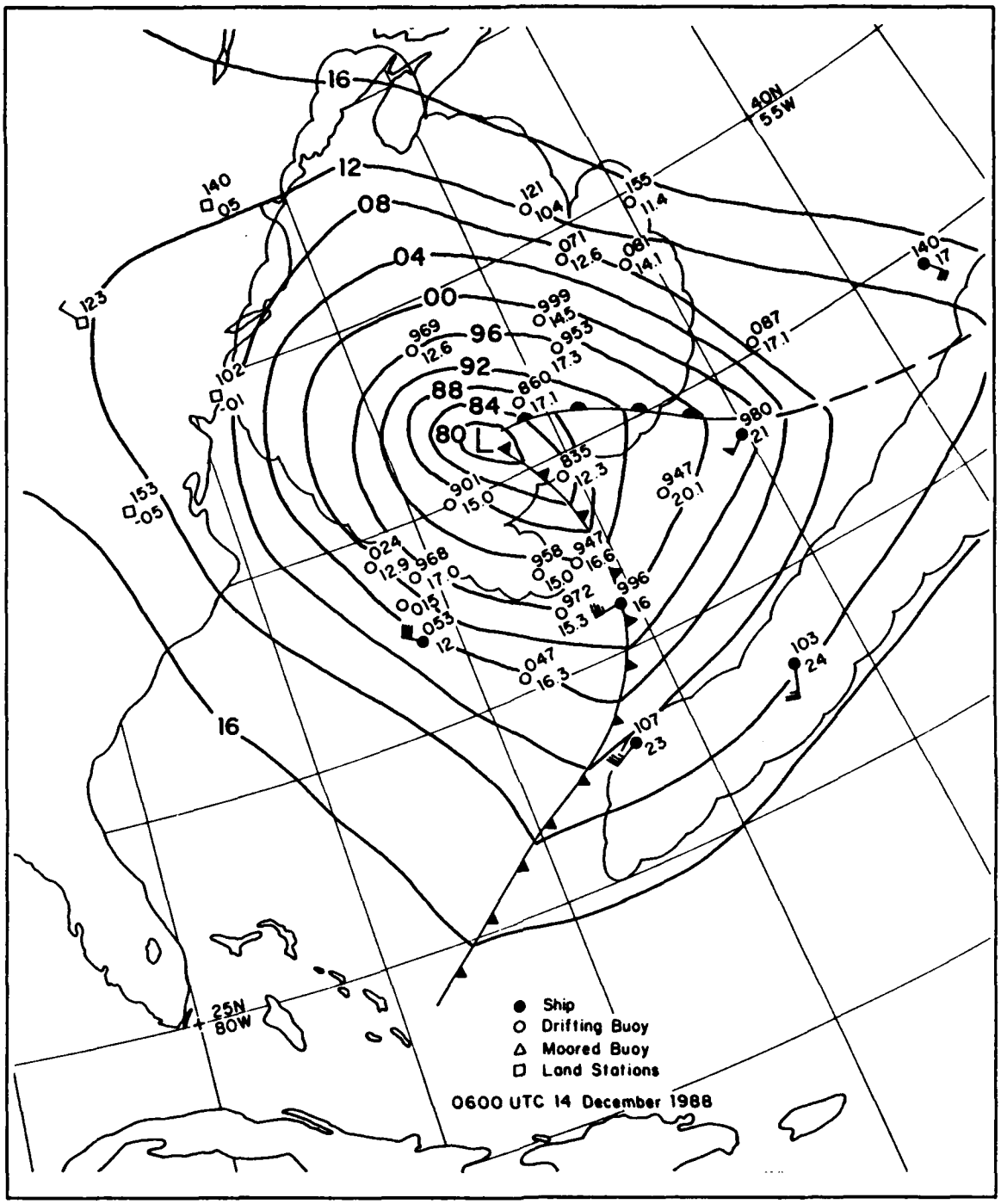

Figure 13. As in Figure 2 except for 14/0600 UTC December 1988.

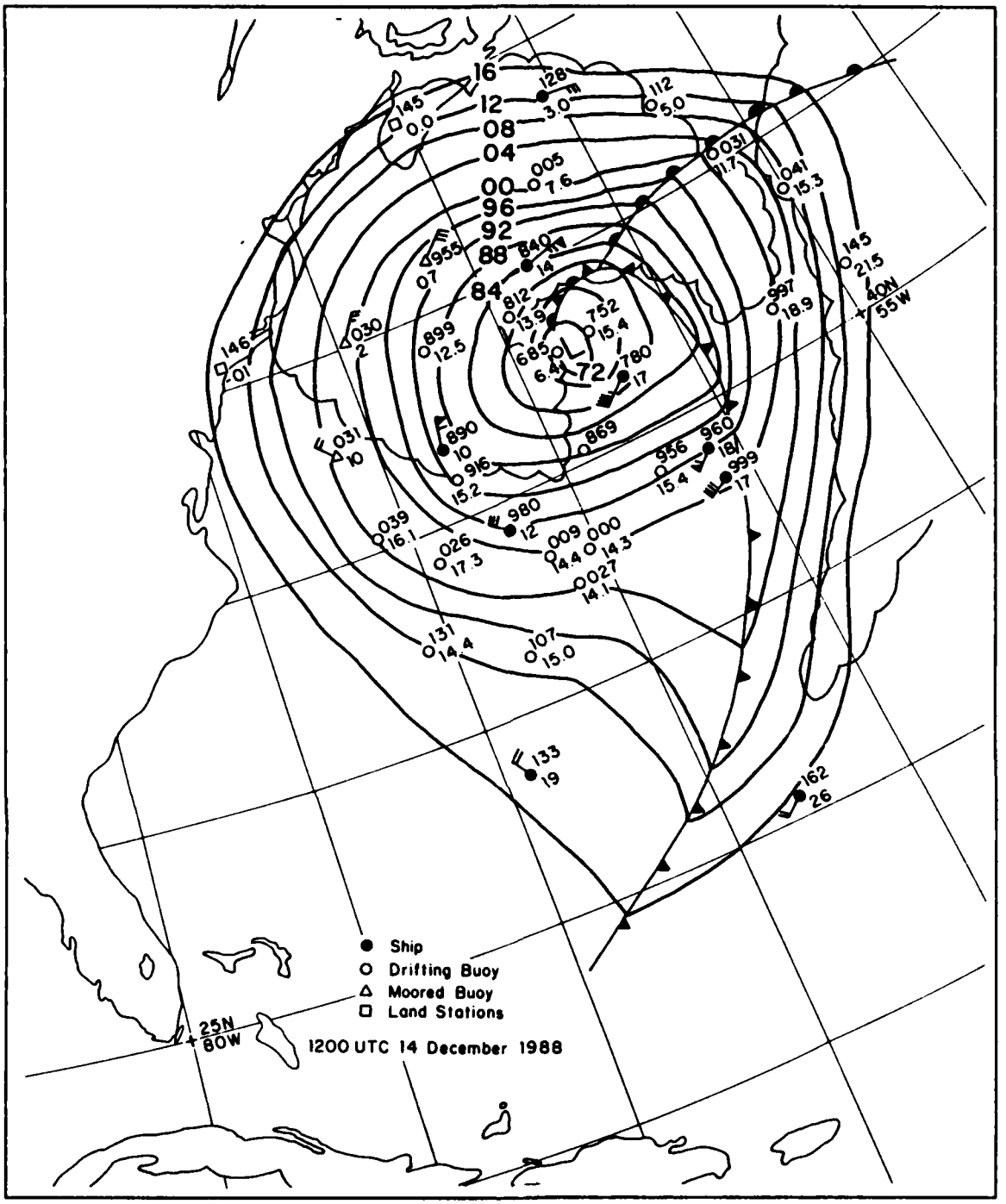

Figure 14. As in Figure 2 except for 14/1200 UTC December 1988.

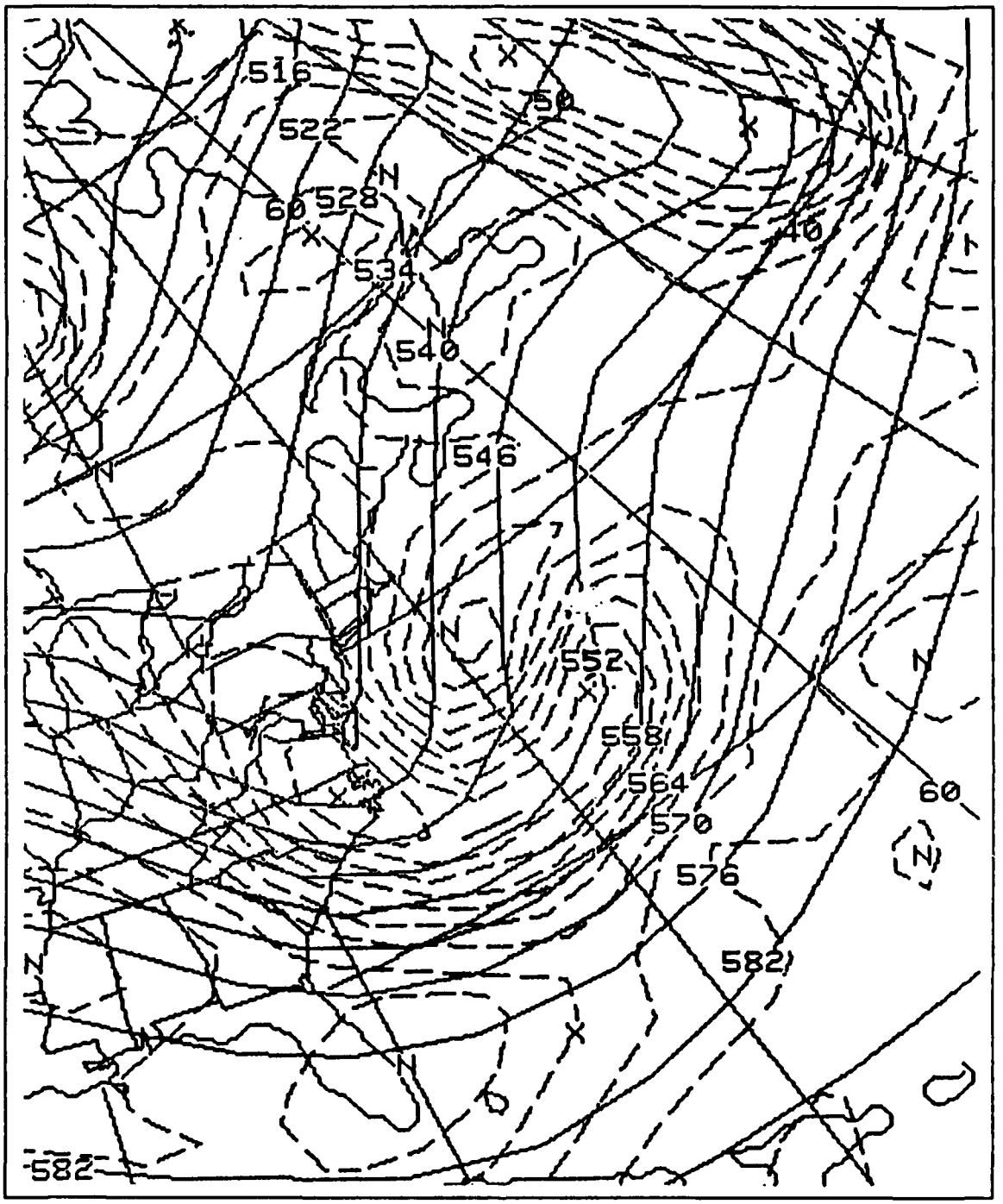

Figure 15. The 500 mb NMC Spectral 24-h model forecast valid 14/0000 UTC December 1988.

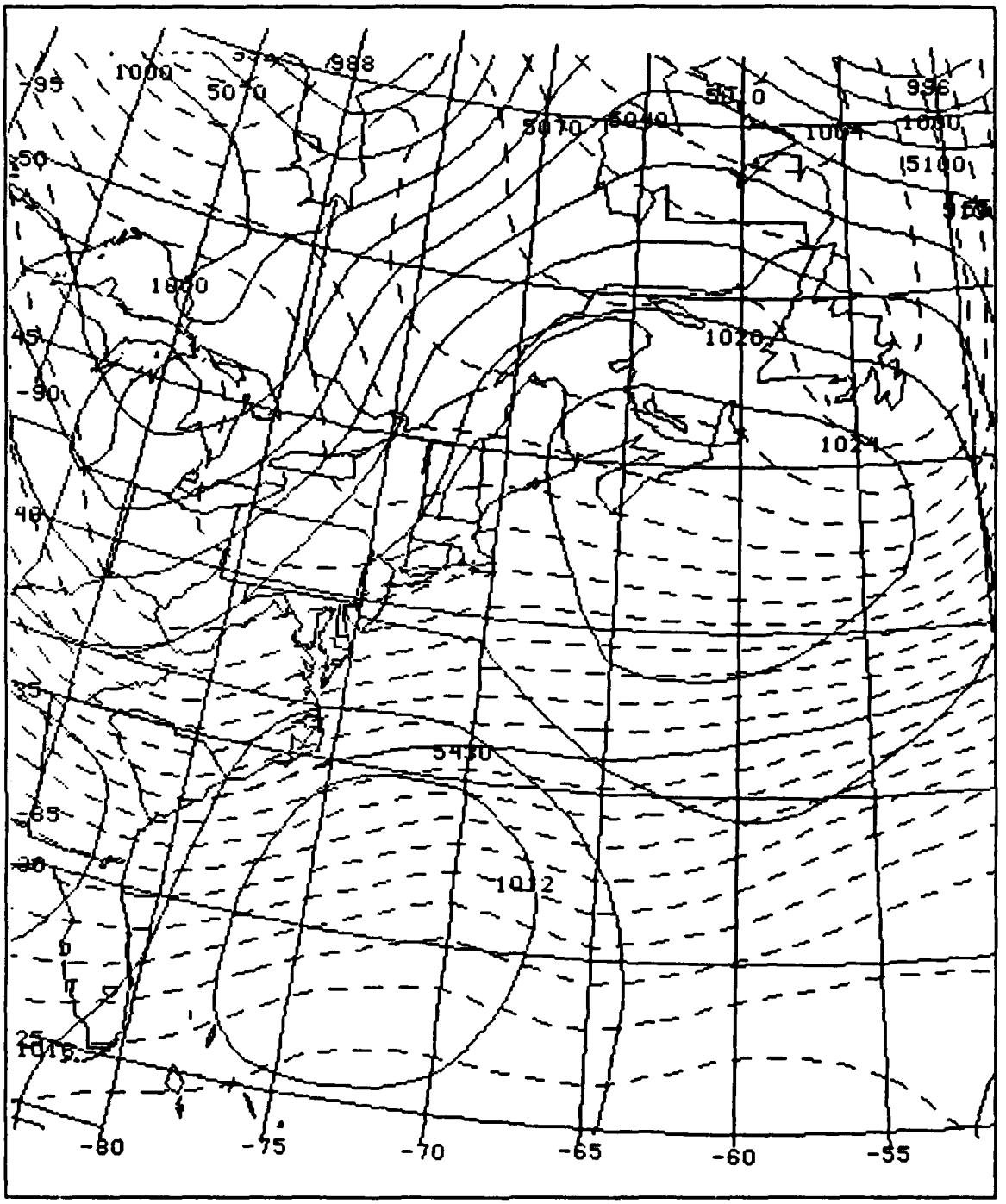

Figure 16. NMC operational global optimal interpolation analysis for 13/1200 UTC December 1988 of MSL pressure (mb, solid) and 1000-500 thickness (m, dashed).

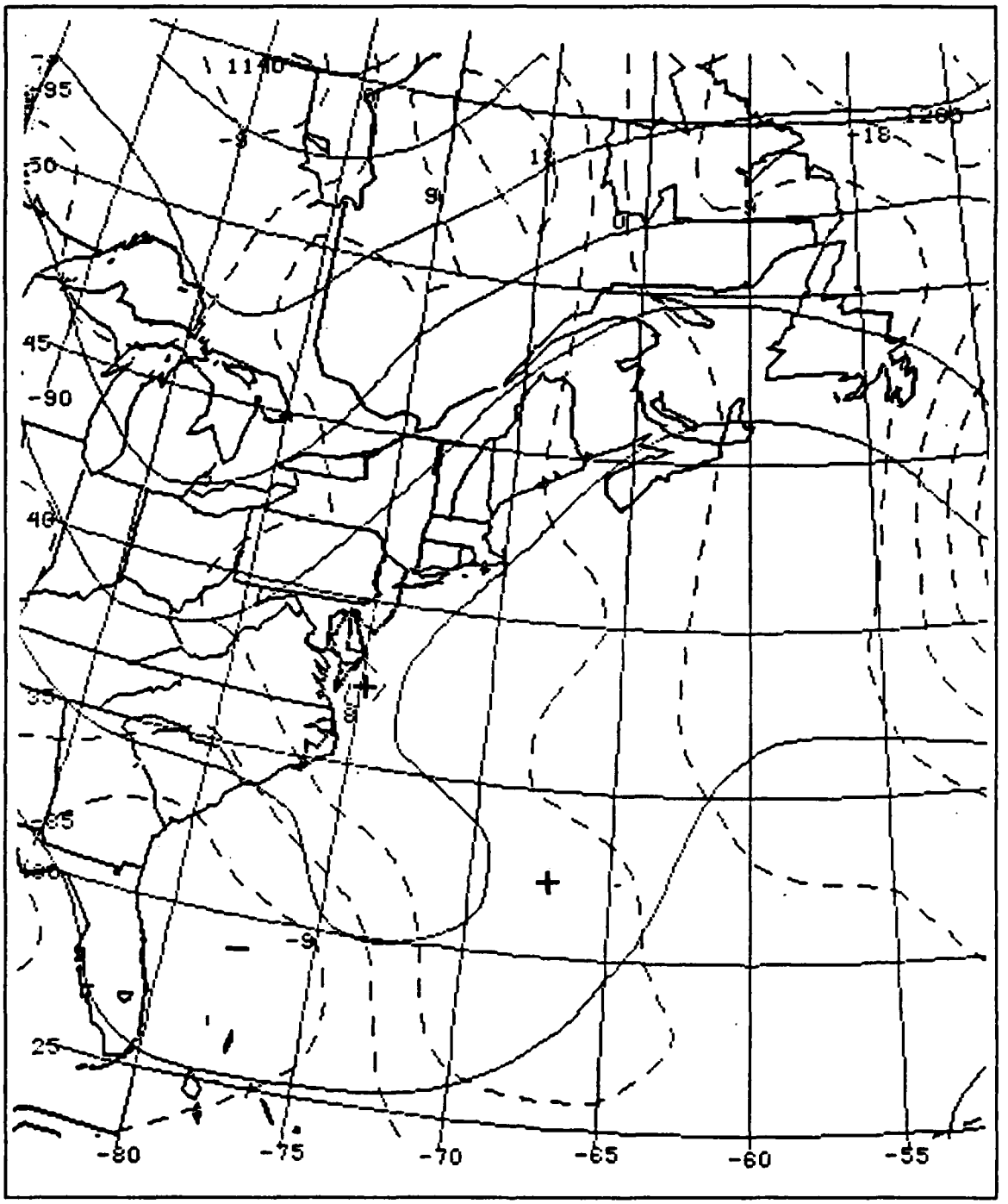

Figure 17. NMC operational 850 mb interpolation analyses for 13/1200 UTC December 1988 of geopotential height (m, solid) and thermal advection (K/sec $\times 10^{-5}$,dashed).for

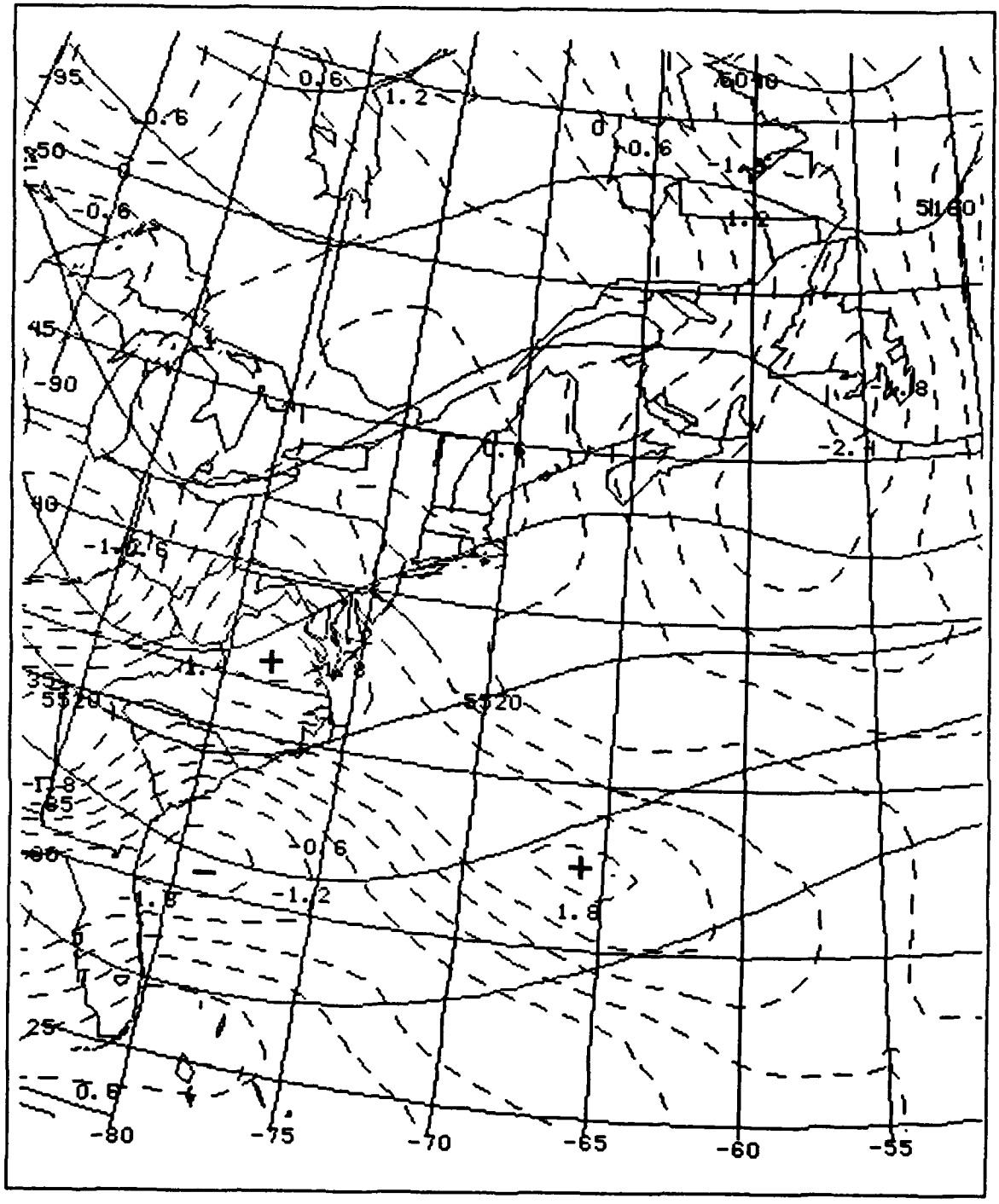

Figure 18. NMC operational interpolation analyses for 13/1200 UTC December 1988 of vorticity advection ($s^{-2} \times 10^{-9}$, dashed) and geopotential height (m, solid) for 13/1200 December 1988.

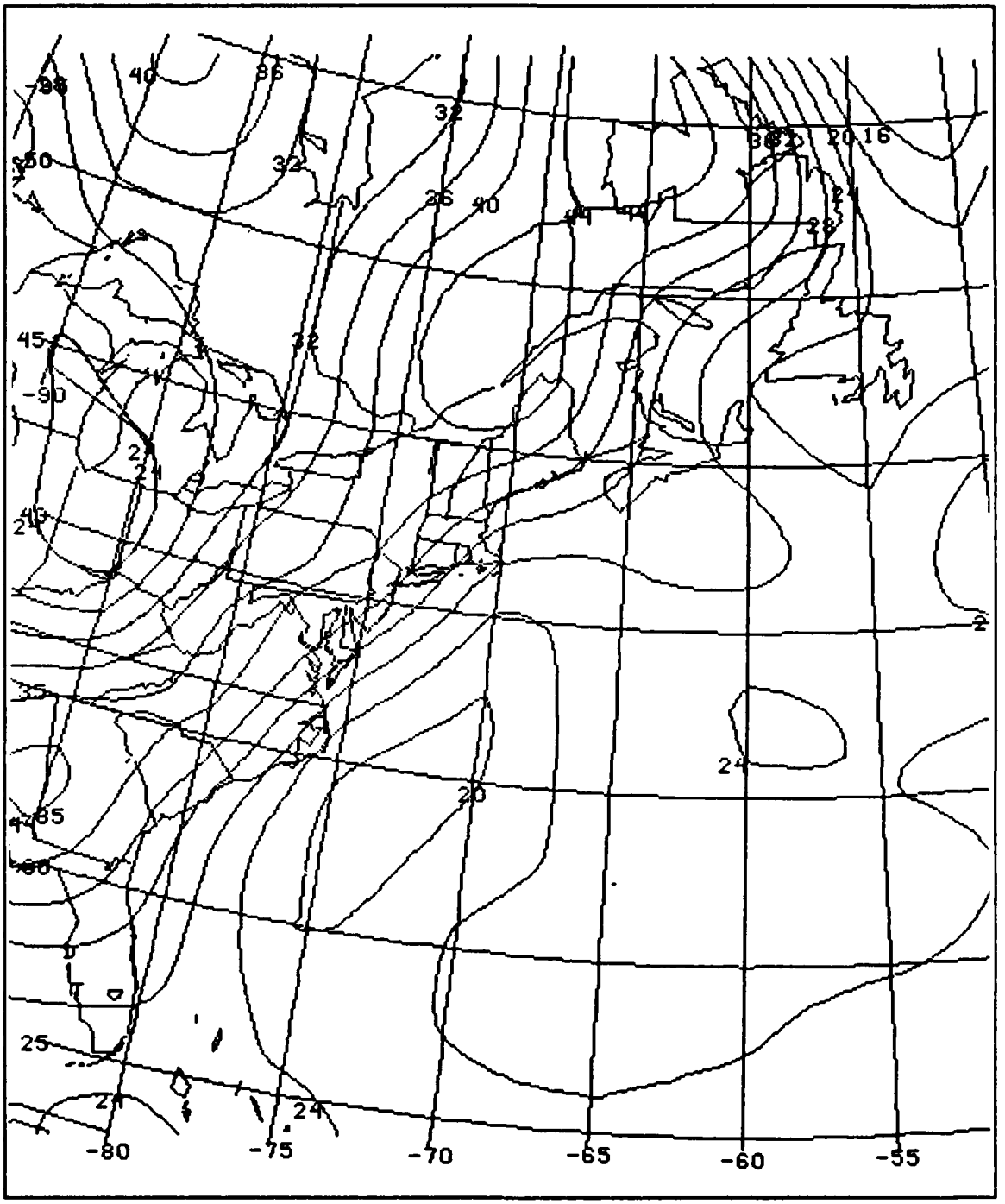

Figure 19. NMC operational interpolation analyses for 13/1200 UTC December of static stability (K/500 mb, solid).

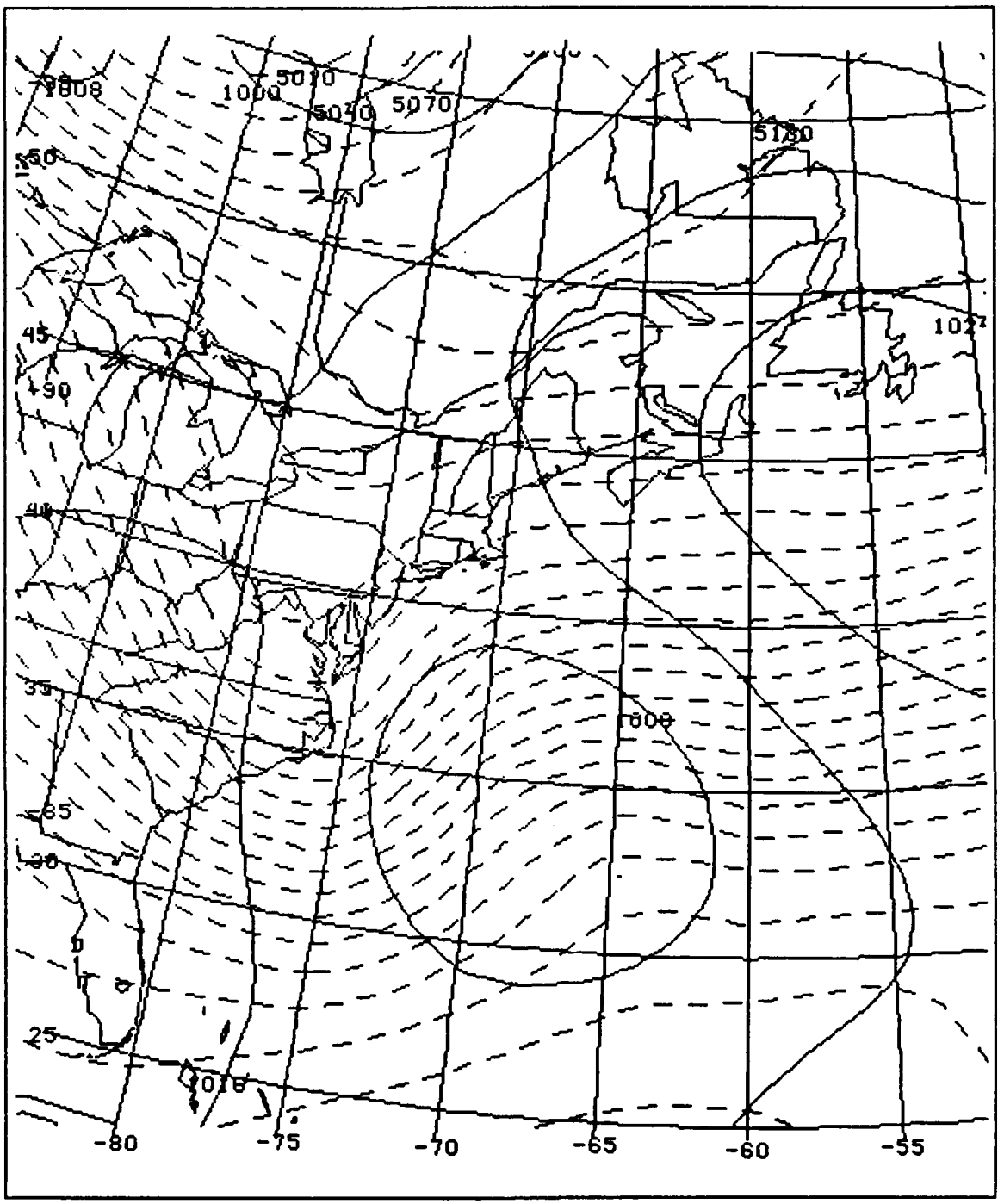

Figure 20. As in Figure 16 except for 14/0000 UTC December 1988.

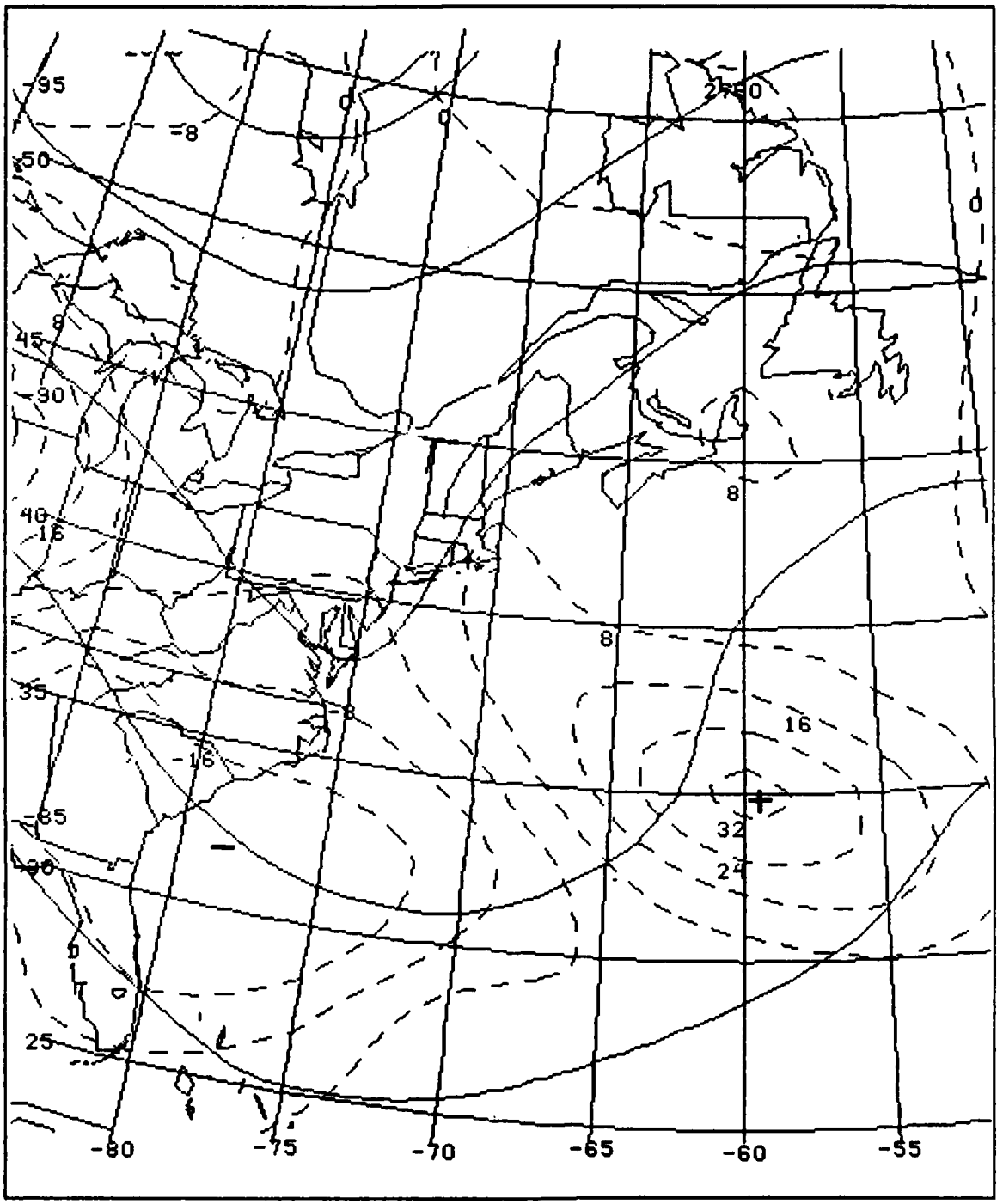

Figure 21. As in Figure 17 except 700 mb for 14/0000 UTC December 1988.

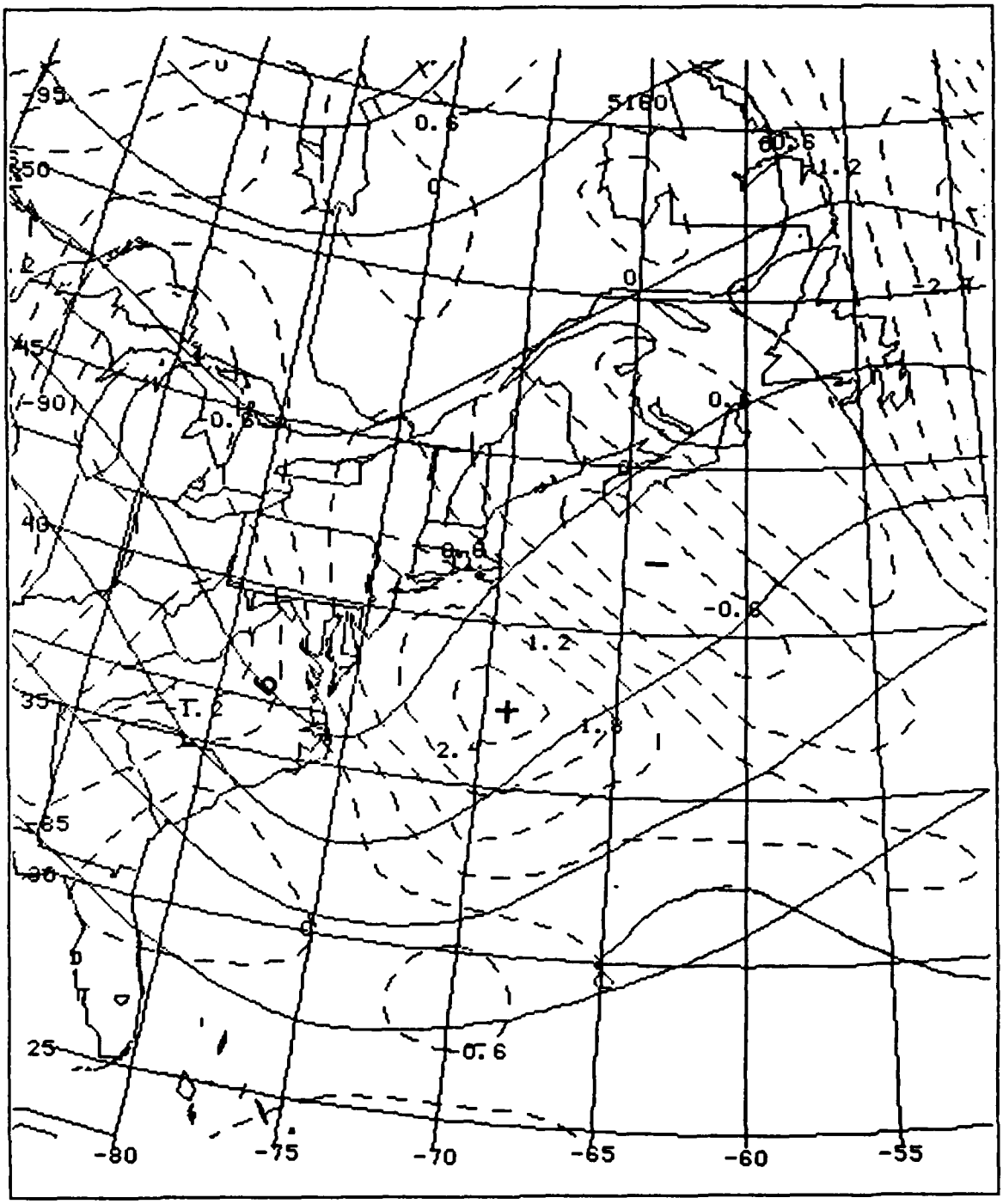

Figure 22. As in Figure 18 except for 14/0000 UTC December 1988.

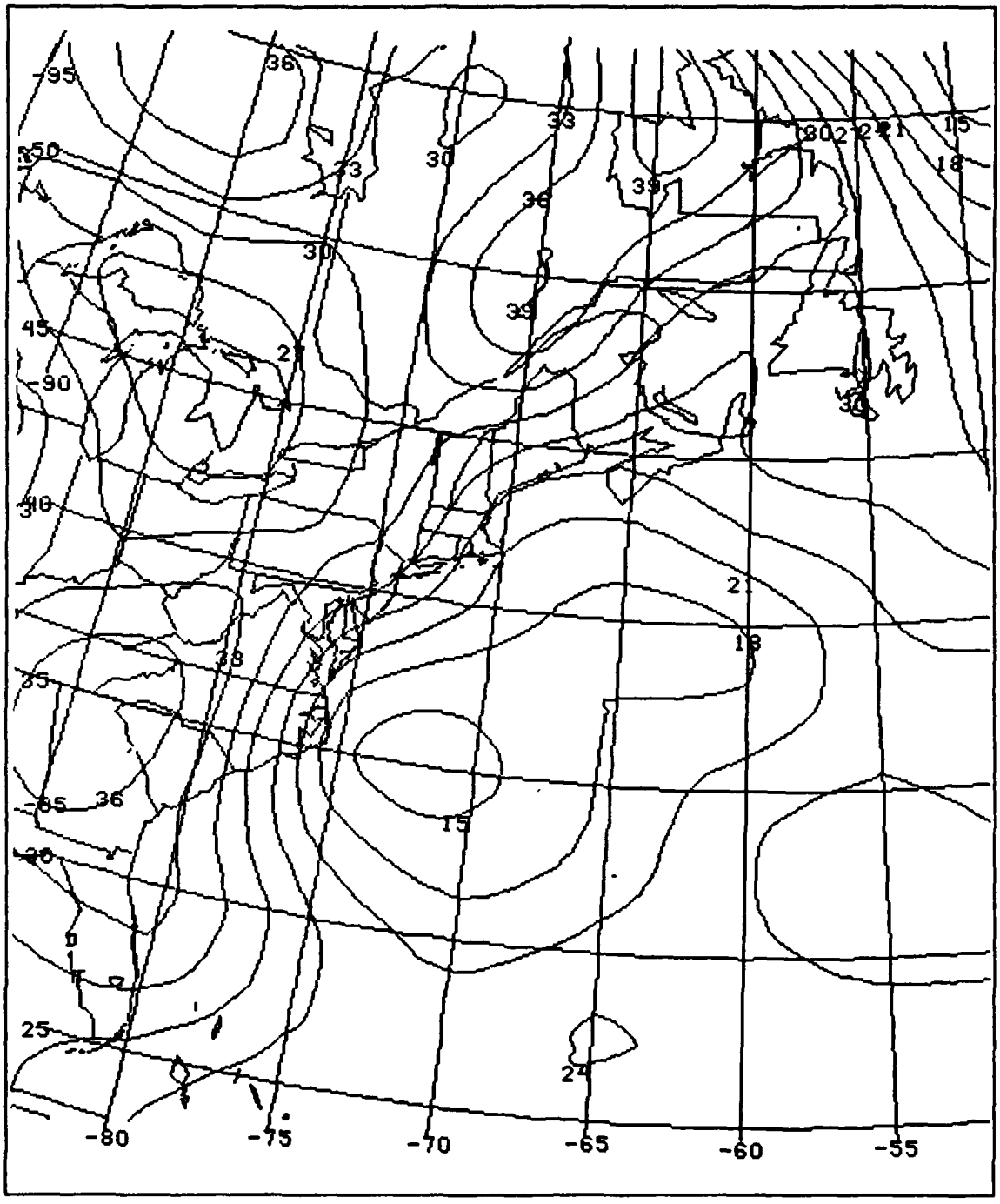

Figure 23. As in Figure 19 except for 14/0000 UTC December 1988.

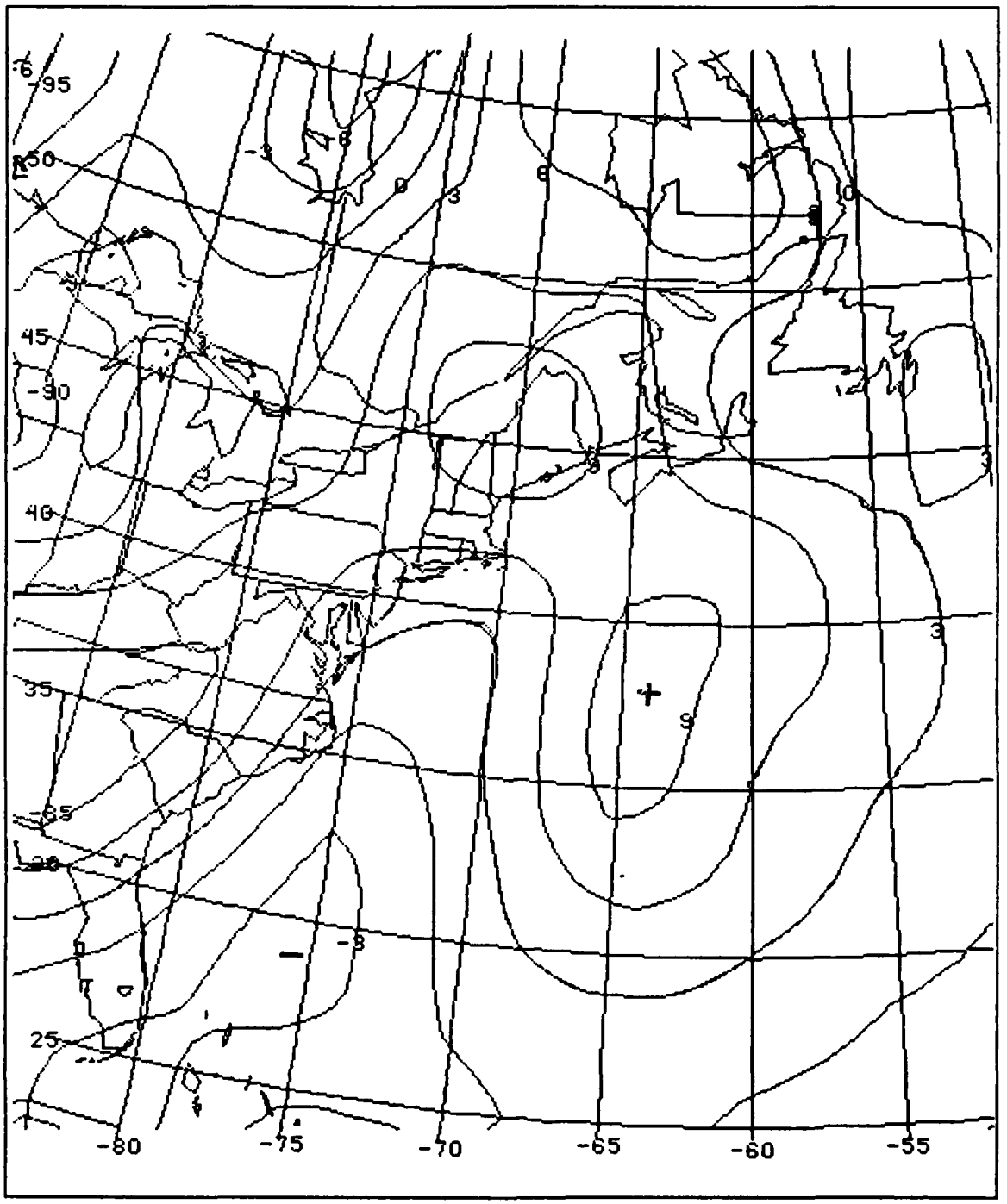

Figure 24. NMC operational optimal interpolation analyses of 12-h temperature change (K, dashed) and geopotential height (m, solid) for 13/1200 UTC to 14/0000 UTC December 1988.

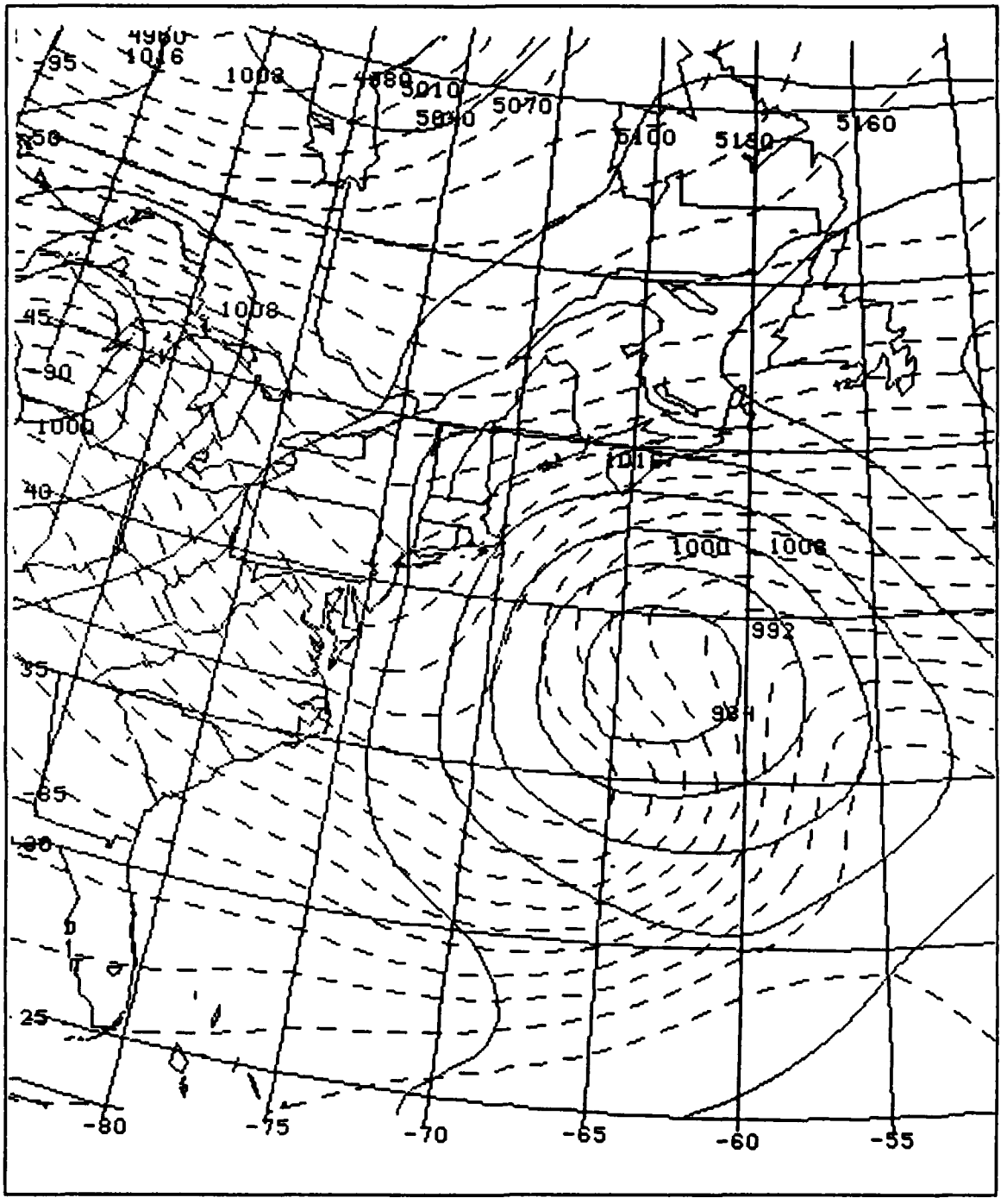

Figure 25. As in Figure 16 except for 14/1200 UTC December 1988.

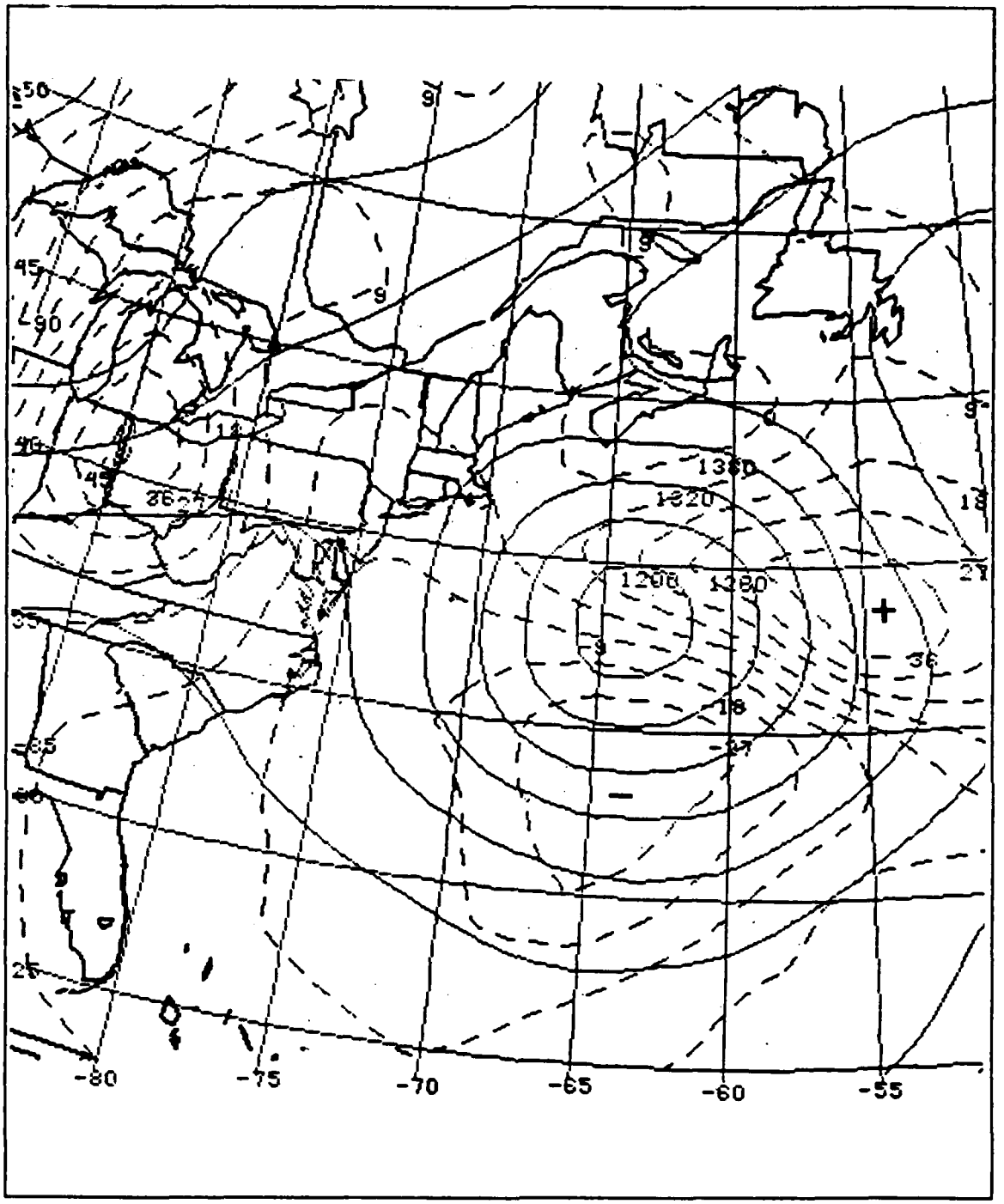

Figure 26. As in Figure 17 except for 14/1200 UTC December 1988.

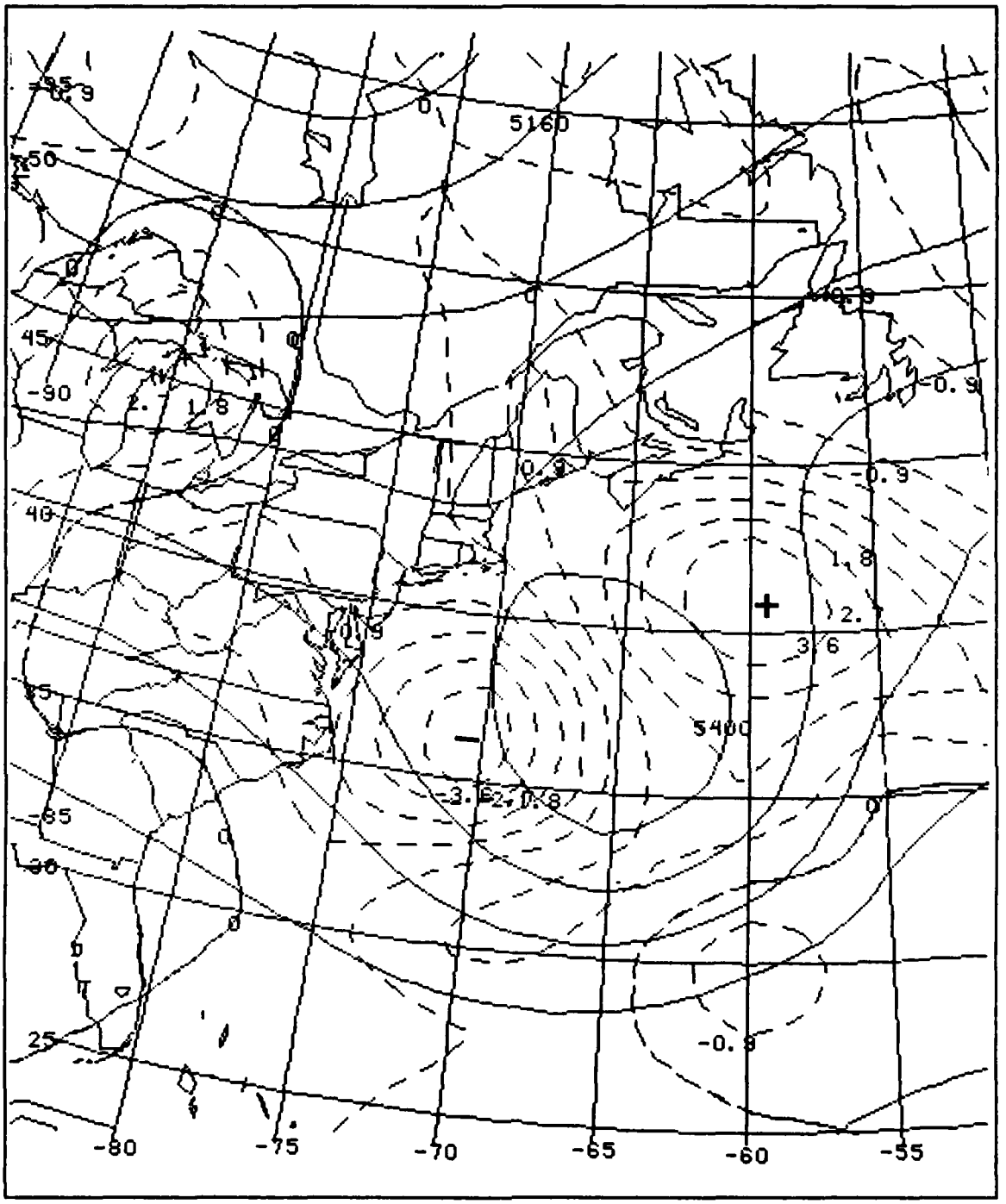

Figure 27. As in Figure 18 except for 14/1200 UTC December 1988.

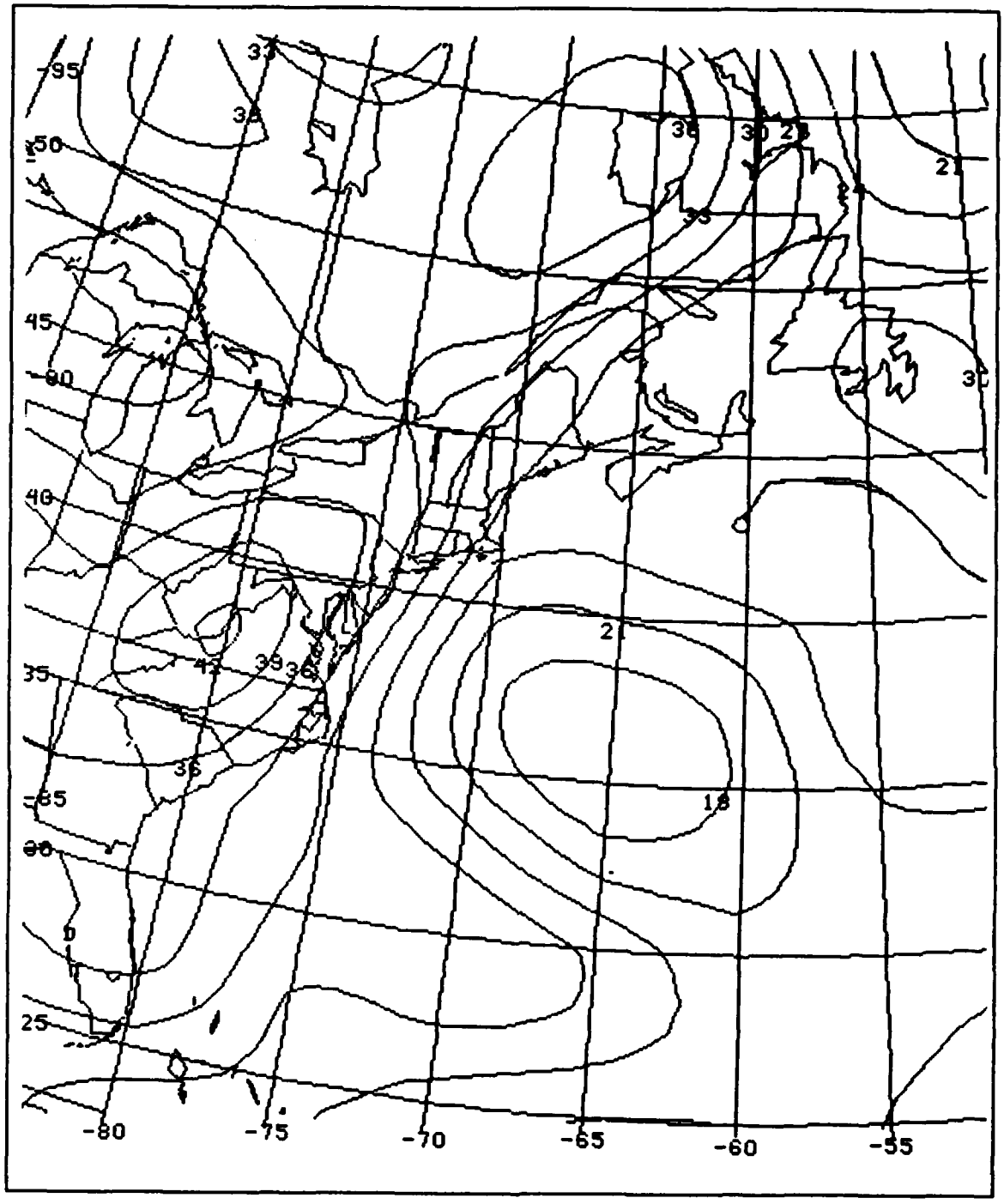

Figure 28. As in Figure 19 except for 14/1200 UTC December 1988.

LIST OF REFERENCES

Dirks, R. A., J. P. Kuettner and J. A. Moore, 1988: Genesis of Atlantic Lows Experiment (GALE): An Overview. *Bull. of Amer. Meteor. Soc.* , **69**, 148-160.

Hadlock, R., 1988: *Experiment on Rapid Intensification of Cyclones over the Atlantic (ERICA) Field Operations Plan.* ERICA Project Office, Battelle Ocean Sciences, Richland, Washington, 280pp.

Hartnett, E., G. Forbes and R. Hadlock, 1989: *Experiment on Rapid Intensification of Cyclones over the Atlantic (ERICA) Field Phase Summary.* Department of Physics and Atmospheric Science, Drexel University, Philadelphia, PA, 300pp.

Holton, J. R., 1979:*An Introduction to Dynamic Meteorology.* Academic Press,Inc., New York, 136-137.

Sanders, F., 1987: Skill of NMC operational dynamical models in prediction of explosive cyclogenesis. *Weather and Forecasting*, **2**, 322-336.

------- and J. R. Gyakum, 1980: Synoptic-dynamic climatology of the 'bomb'. *Mon. Wea. Rev.*, **108**, 1589-1606.

Uccellini, L. W., 1989: Processes contributing to the rapid development of extratropical cyclones. *Proceedings of Palmen Memorial Symposium on Extratropical Cyclones.* Helsinki, Finland, August 1988. American Meteorological Society, in press.

Wash, C. H., J. E. Peak, W. E. Calland and W. A. Cook, 1988: Diagnostic study of explosive cyclogenesis during FGGE. *Mon. Wea. Rev.*, **116**, 431-451.

INITIAL DISTRIBUTION LIST

		No. Copies
1.	Defense Technical Information Center Cameron Station Alexandria, VA 22304-6145	2
2.	Library, Code 0142 Naval Postgraduate School Monterey, CA 93943-5002	2
3.	Commander Naval Oceanography Command Stennis Space Center, MS 39529-5000	1
4.	Commanding Officer Naval Oceanography Office Stennis Space Center, MS 39529-5001	1
5.	Commanding Officer Naval Ocean Research and Development Activity Stennis Space Center, MS 39529-5004	1
6.	Commanding Officer Fleet Numerical Oceanography Center Monterey, CA 93943-5005	1
7.	Commanding Officer Air Force Global Weather Center Offutt Air Force Base, NE 68113	1
8.	Officer-in-Charge Naval Environment Prediction Research Facility Monterey, CA 93943-5006	1
9.	Prof. R.J. Renard, Code 63Rd Department of Meteorology Naval Postgraduate School Monterey, CA 93943-5000	1
10.	USAF ETAC/LD Air Weather Service Technical Library Scott Air Force Base, IL 62225	1
11.	Professor Carlyle H. Wash (Code 63Wx) Department of Meteorology Naval Postgraduate School Monterey, CA 93943-5000	8

12. Professor Wendell A. Nuss (Code 63Nu) — 1
Department of Meterology
Naval Postgraduate School
Monterey, CA 93943-5000

13. Captain Amy E. Chalfant — 1
Detachment 2, 2 WS
Hanscom AFB NE 01731-5000

14. Commanding Officer — 1
Naval Environmental Prediction Research Facility
Monterey, CA 93943-5006

15. Director Naval Oceanography Division — 1
Naval Observatory
34th and Massachusetts Avenue NW
Washingtion, DC 20390

16. Chairman, Oceanography Department — 1
U.S. Naval Academy
Annapolis, MD 21402

17. Chief of Naval Research — 1
800 N. Quincy Street
Arlingtion, VA 22217

18. Commander — 1
Air Weather Service
Scott AFB, IL 62225